AD-A043 295 COMPUTER CODE CONSULTANTS SOLANA BEACH CALIF F/G 19/4
THREE-DIMENSIONAL COMPUTATIONS. VOLUME I: 30 DEG OBLIQUE IMPACT--ETC(U)
JUL 77 W JOHNSON, V KUCHER DAAD05-76-C-0755
UNCLASSIFIED BRL-CR-344 NL

| OF |
AD
A043295

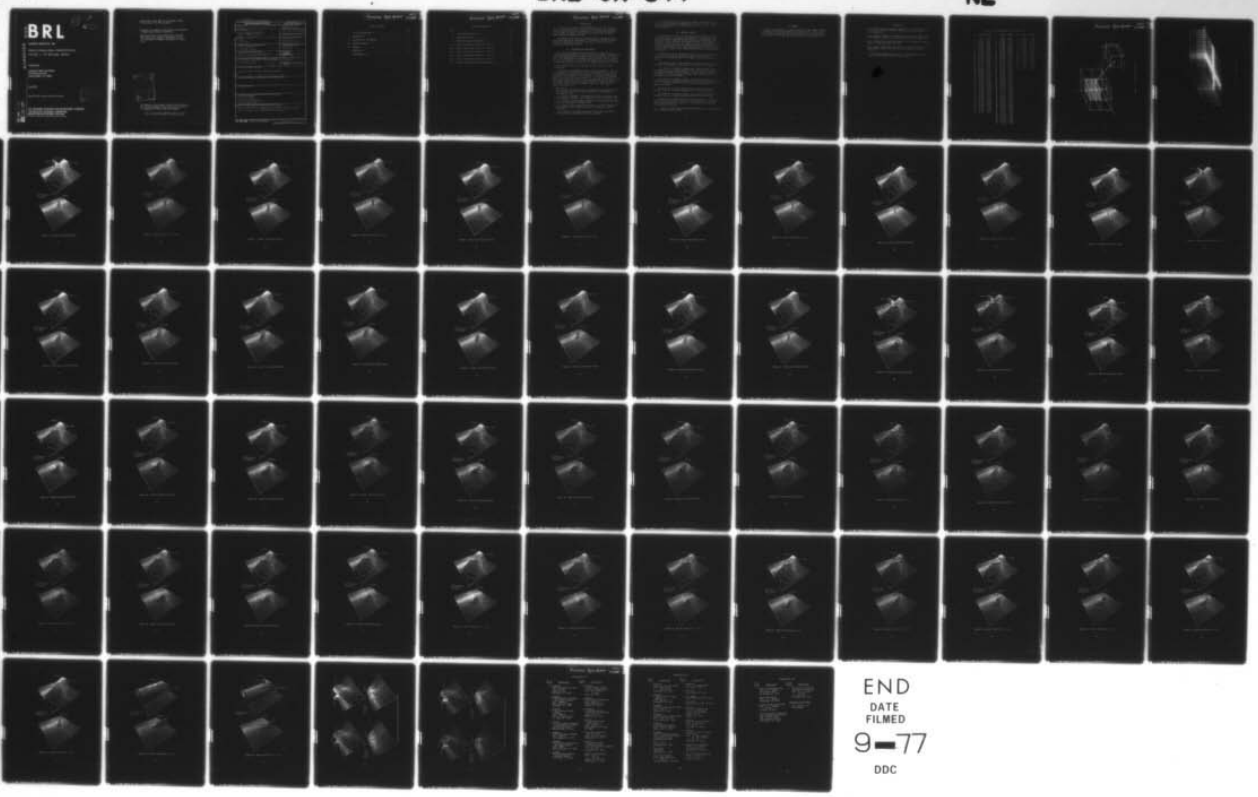

END
DATE
FILMED
9-77
DDC

BRL CR 344

BRL

AD

CONTRACT REPORT NO. 344

THREE-DIMENSIONAL COMPUTATIONS, VOLUME I: 30° OBLIQUE IMPACT

Prepared by

Computer Code Consultants
527 Glencrest Drive
Solana Beach, CA 92075

July 1977

Approved for public release; distribution unlimited.

USA ARMAMENT RESEARCH AND DEVELOPMENT COMMAND
USA BALLISTIC RESEARCH LABORATORY
ABERDEEN PROVING GROUND, MARYLAND

Destroy this report when it is no longer needed.
Do not return it to the originator.

Secondary distribution of this report by originating or sponsoring activity is prohibited.

Additional copies of this report may be obtained from the National Technical Information Service, U.S. Department of Commerce, Springfield, Virginia 22151.

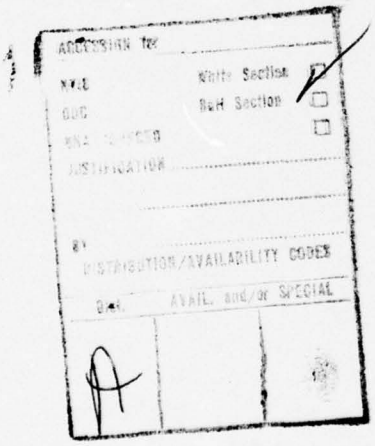

The findings in this report are not to be construed as an official Department of the Army position, unless so designated by other authorized documents.

The use of trade names or manufacturers' names in this report does not constitute indorsement of any commercial product.

UNCLASSIFIED

SECURITY CLASSIFICATION OF THIS PAGE (When Data Entered)

REPORT DOCUMENTATION PAGE

READ INSTRUCTIONS BEFORE COMPLETING FORM

1. REPORT NUMBER: BRL Contract Report No. 344
2. GOVT ACCESSION NO.:
3. RECIPIENT'S CATALOG NUMBER:

4. TITLE (and Subtitle): THREE-DIMENSIONAL COMPUTATIONS, VOLUME I. 30° OBLIQUE IMPACT.
5. TYPE OF REPORT & PERIOD COVERED: Final, April 1976-April-1977
6. PERFORMING ORG. REPORT NUMBER:

7. AUTHOR(s): W. Johnson, V. Kucher (BRL)
8. CONTRACT OR GRANT NUMBER(s): DAAD05-76-C-0755

9. PERFORMING ORGANIZATION NAME AND ADDRESS: Computer Code Consultants, 527 Glencrest Drive, Solana Beach, CA 92075
10. PROGRAM ELEMENT, PROJECT, TASK AREA & WORK UNIT NUMBERS: 1W161102A33H

11. CONTROLLING OFFICE NAME AND ADDRESS: USARRADCOM, Ballistic Research Laboratory, Aberdeen Proving Ground, MD 21005
12. REPORT DATE: JULY 1977
13. NUMBER OF PAGES: 81

14. MONITORING AGENCY NAME & ADDRESS (if different from Controlling Office): US Army Materiel Development & Readiness Command, 5001 Eisenhower Avenue, Alexandria, VA 22333
15. SECURITY CLASS. (of this report): UNCLASSIFIED
15a. DECLASSIFICATION/DOWNGRADING SCHEDULE:

16. DISTRIBUTION STATEMENT (of this Report)

Approved for public release; distribution unlimited.

Final rept. Apr 76 - Apr 77

17. DISTRIBUTION STATEMENT (of the abstract entered in Block 20, if different from Report)

18. SUPPLEMENTARY NOTES

19. KEY WORDS (Continue on reverse side if necessary and identify by block number)

Penetration mechanics
Hypervelocity impact
Hydrodynamic computer code
Three-dimensional computer code
Eulerian computer code

20. ABSTRACT (Continue on reverse side if necessary and identify by block number) dj

Numerical computations were made in 1975 of four oblique impact problems: 30°, 45°, 60°, and 77.5°. A graphical display of the results of the 30° impact of a copper jet on a steel target are presented.

DD FORM 1 JAN 73 1473 EDITION OF 1 NOV 65 IS OBSOLETE

UNCLASSIFIED 341 758

SECURITY CLASSIFICATION OF THIS PAGE (When Data Entered)

TABLE OF CONTENTS

LIST OF ILLUSTRATIONS

I. INTRODUCTION

A series of four oblique impact computations (30°, 45°, 60°, and 77.5°) involving a copper jet impacting a steel plate were completed in 1975 for the Ballistic Research Laboratory.[1] This work was performed using TRIDORF[2] and DORF[3,4] and ancillary programs CUBIT[3] and ADJUST[3] under Contract No. DAAD05-75-C-0738.

The effort for 1976 has been directed towards a graphical display of the data from these computations. The results of the 30° obliquity impact are reported here; the 45°, 60°, and 77.5° obliquities are presented in sequential volumes.

II. DESCRIPTION OF THE PROBLEM

The 30° oblique impact computation involved a copper jet with a 0.7086-mm radius impacting on a 12.7-mm thick steel target. The obliquity angle is measured between the normal to the target and the axis of the jet. Since TRIDORF uses a rectangular grid, the copper jet was treated as a bar with a square cross section of 1.256-mm width, thus preserving the cross-sectional area of the jet. The impact velocity was 7.55 km/s.

The Tillotson[5] form of the equation of state was used for the calculations.

A view of a three-dimensional grid is shown in Figure 1. Each cell is identified by the coordinates (I,J,K), which number the cells in the x,y,z-directions, respectively. The overall size of the computational grid was x = 39.256 mm by y = 40.270 mm by z = 17.539 mm. The maximum number of cells in the x-direction was I = 42, in the y-direction, J = 48, and in the z-direction, K = 18. The total number of cells in the grid was 36,288. Table I presents the dimensions of the cells, DX, DY, and DZ, and the grid coordinates as shown in Figure 1. These data are displayed in Figure 2.

---

1. W. E. Johnson, "Three-Dimensional Computations on Penetrator-Target Interactions," Ballistic Research Laboratory Contractor Report No. 338, May 1977.
2. W. E. Johnson, "TRIDORF - A Two-Material Version of the TRIOIL Code with Strength," Computer Code Consultants, CCC-976, September 1976.
3. W. E. Johnson, "Code Correlation Study," Air Force Weapons Laboratory Report No. AFWL-TR-70-144, April 1971.
4. W. E. Johnson, "Development and Application of Computer Programs to Hypervelocity Impact," Systems, Science and Software, 3SR-749, July 1971.
5. J. H. Tillotson, "Metallic Equations of State for Hypervelocity Impact," Gulf General Atomic, GA-3216, July 1962.

The xy-plane was used as a plane of symmetry through the bar in order to keep the number of computational cells at a minimum. Figure 3 shows the penetrator-target configuration as it was located in the computational grid.

III. GRAPHICAL RESULTS

The numerical output of the computations are presented as density and pressure fields. The density and pressure are plotted on a two-dimensional spatial plane having the coordinates corresponding to the centers of cells. The fields are plotted such that a cell-number coordinate is held constant. For example, K may be constant meaning that the density or pressure is being presented for the cells between two z-planes bounding the K-cells. These bounding planes will be indicated in each figure. Figures 2 and 3 should be useful for orienting oneself in the grid.

The density scale for the density field plots can be realized from the initial density of the jet and the target, 8.9 and 7.8 Mg/m^3, respectively. The density scale is the same in all the density field plots.

The pressure scale is not the same in all the pressure field plots; therefore, the maximum pressure, Pmax, is indicated on each figure.

The first set of figures, Figures 4-15, shows the density and pressure fields at a constant time of 0.629 μs for various K-slabs which are numbered from the plane of symmetry. The jet appears distinctly only when K = 1 and K = 2 since, initially, the jet was two cells in width from the plane of symmetry.

The second set of figures, Figures 16-26, shows the density and pressure fields at a constant time of 1.34 μs for various K-slabs. Data for K = 6, 9, and 10 could not be recovered from the magnetic output tapes for plotting.

The third set of figures, Figures 27-44, shows the density and pressure fields at a constant time of 2.84 μs for various K-slabs.

The fourth set of figures, Figures 45-61, shows the density and pressure fields at a constant time of 3.60 μs for various K-slabs.

Figures 62-63 show the density and pressure fields at a constant time of 2.84 μs for slabs I = 10 and I = 21, respectively. Note that the jet appears distinctly only for I = 21 since this slab initially contained part of the jet.

A comparison of the density and pressure fields at K = 1 for various times is shown in Figures 64-65.

IV. SUMMARY

Numerical computations were made in 1975 of oblique impact problems. A graphical display of the results of the 30° impact of a copper jet on a steel target are presented for future analysis. The results for the 30°, 60°, and 77.5° oblique impacts are presented in sequential volumes.

REFERENCES

1. W. E. Johnson, "Three-Dimensional Computations on Penetrator-Target Interactions," Ballistic Research Laboratory Contractor Report No. 338, May 1977.

2. W. E. Johnson, "TRIDORF - A Two-Material Version of the TRIOIL Code with Strength," Computer Code Consultants, CCC-976, September 1976.

3. W. E. Johnson, "Code Correlation Study," Air Force Weapons Laboratory Report No. AFWL-TR-70-144, April 1971.

4. W. E. Johnson, "Development and Application of Computer Programs to Hypervelocity Impact," Systems, Science and Software, 3SR-749, July 1971.

5. J. H. Tillotson, "Metallic Equations of State for Hypervelocity Impact," Gulf General Atomic, GA-3216, July 1962.

Table I. Grid Coordinates and Cell Dimensions

I	x (mm)	DX (mm)	J	y (mm)	DY (mm)	K	z (mm)	DZ (mm)
1	4.730	4.730	1	6.990	6.990	1	0.314	0.314
2	6.847	2.117	2	8.790	1.800	2	0.628	0.314
3	8.541	1.694	3	10.390	1.000	3	0.942	0.314
4	9.896	1.355	4	11.790	1.400	4	1.256	0.314
5	10.980	1.084	5	12.990	1.200	5	1.601	0.345
6	11.965	0.985	6	13.990	1.000	6	1.981	0.380
7	12.861	0.896	7	14.790	0.800	7	2.399	0.418
8	13.675	0.814	8	15.390	0.600	8	2.859	0.460
9	14.415	0.740	9	15.890	0.500	9	3.365	0.506
10	15.088	0.673	10	16.290	0.400	10	3.921	0.556
11	15.707	0.619	11	16.604	0.314	11	4.540	0.619
12	16.263	0.556	12	16.918	0.314	12	5.213	0.673
13	16.769	0.506	13	17.232	0.314	13	5.953	0.740
14	17.229	0.460	14	17.546	0.314	14	6.767	0.814
15	17.647	0.418	15	17.860	0.314	15	7.663	0.896
16	18.027	0.380	16	18.174	0.314	16	8.648	0.985
17	18.372	0.345	17	18.488	0.314	17	9.732	1.084
18	18.686	0.314	18	18.802	0.314	18	17.539	7.807
19	19.000	0.314	19	19.116	0.314			
20	19.314	0.314	20	19.430	0.314			
21	19.628	0.314	21	19.744	0.314			
22	19.942	0.314	22	20.058	0.314			
23	20.256	0.314	23	20.372	0.314			
24	20.570	0.314	24	20.686	0.314			
25	20.884	0.314	25	21.000	0.314			
26	21.229	0.345	26	21.314	0.314			
27	21.609	0.380	27	21.628	0.314			
28	22.027	0.418	28	21.973	0.345			
29	22.487	0.469	29	22.353	0.380			
30	22.993	0.506	30	22.771	0.418			
31	23.549	0.556	31	23.231	0.460			
32	24.168	0.619	32	23.737	0.506			
33	24.841	0.673	33	24.293	0.556			
34	25.581	0.740	34	24.912	0.619			
35	26.395	0.814	35	25.585	0.673			
36	27.291	0.896	36	26.325	0.740			
37	28.276	0.985	37	27.139	0.814			
38	29.360	1.084	38	28.035	0.896			
39	30.715	1.355	39	29.020	0.985			
40	32.409	1.694	40	30.104	1.084			
41	34.526	2.117	41	31.459	1.355			
42	39.256	4.730	42	33.153	1.694			
			43	35.270	2.117			
			44	37.700	2.500			
			45	40.270	2.500			
			46	42.770	2.500			
			47	45.270	2.500			
			48	47.770	2.500			

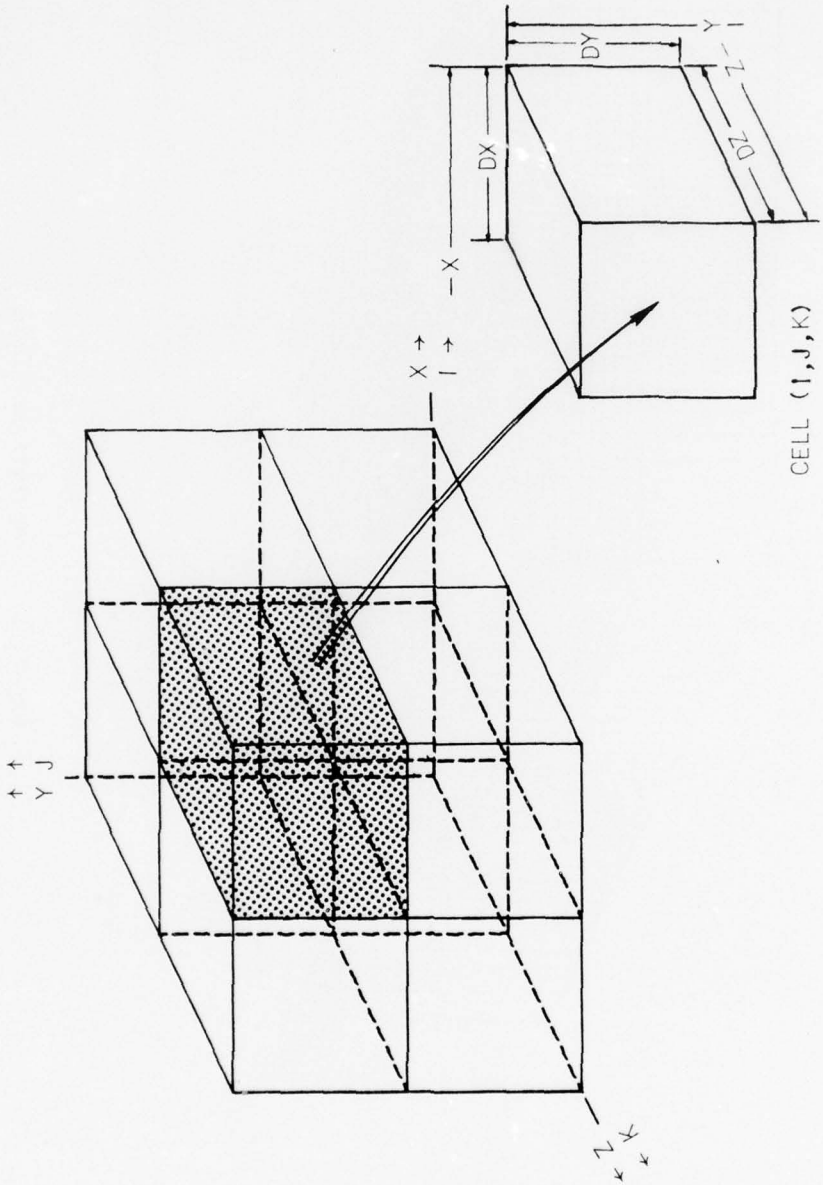

Figure 1. A Three-Dimensional Grid

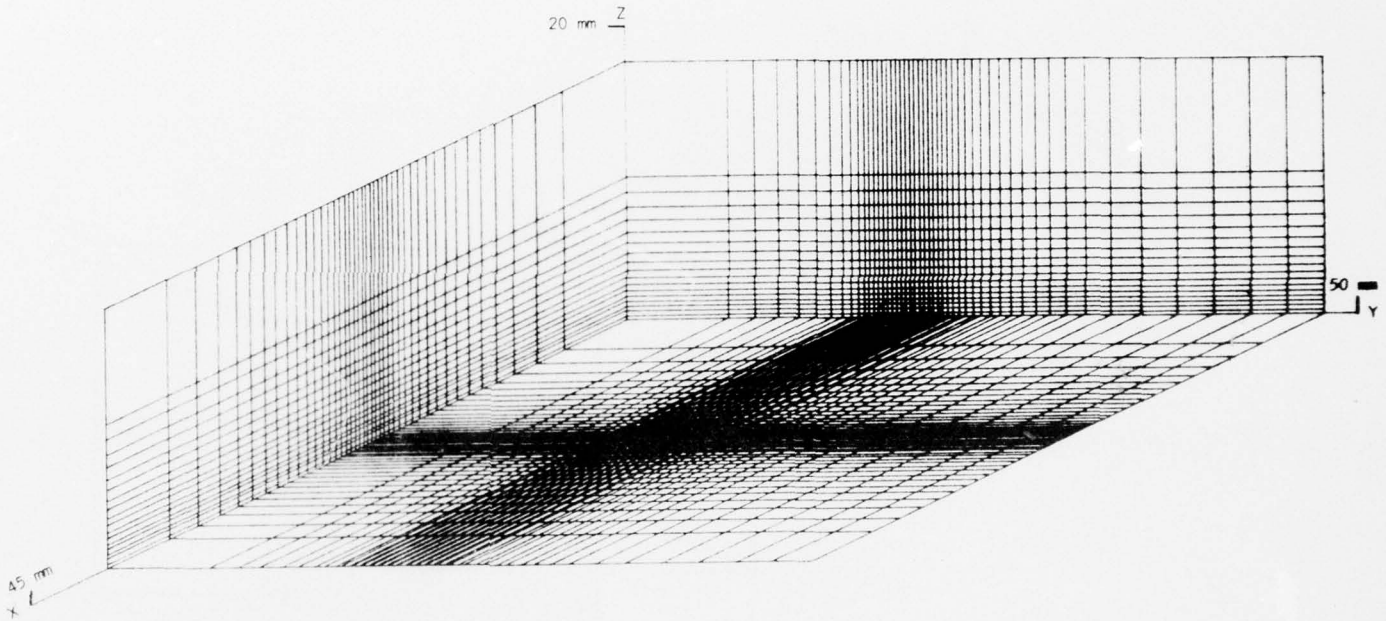

Figure 2. Computational Grid

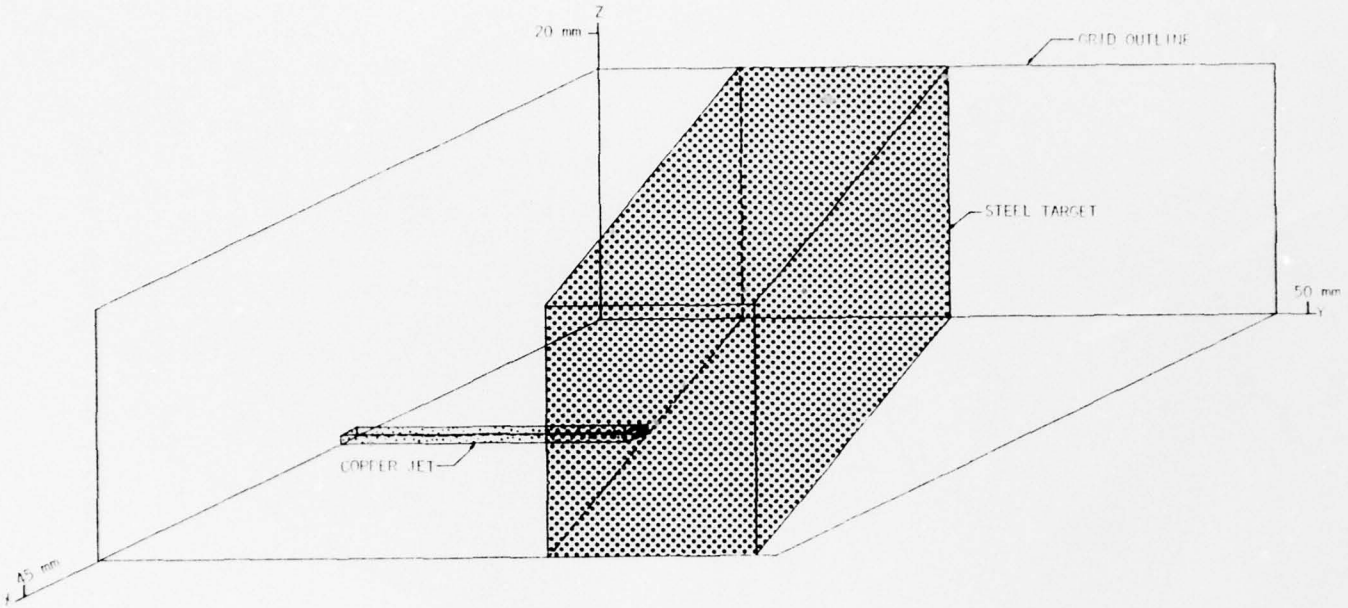

Figure 3. Penetrator-Target Configuration

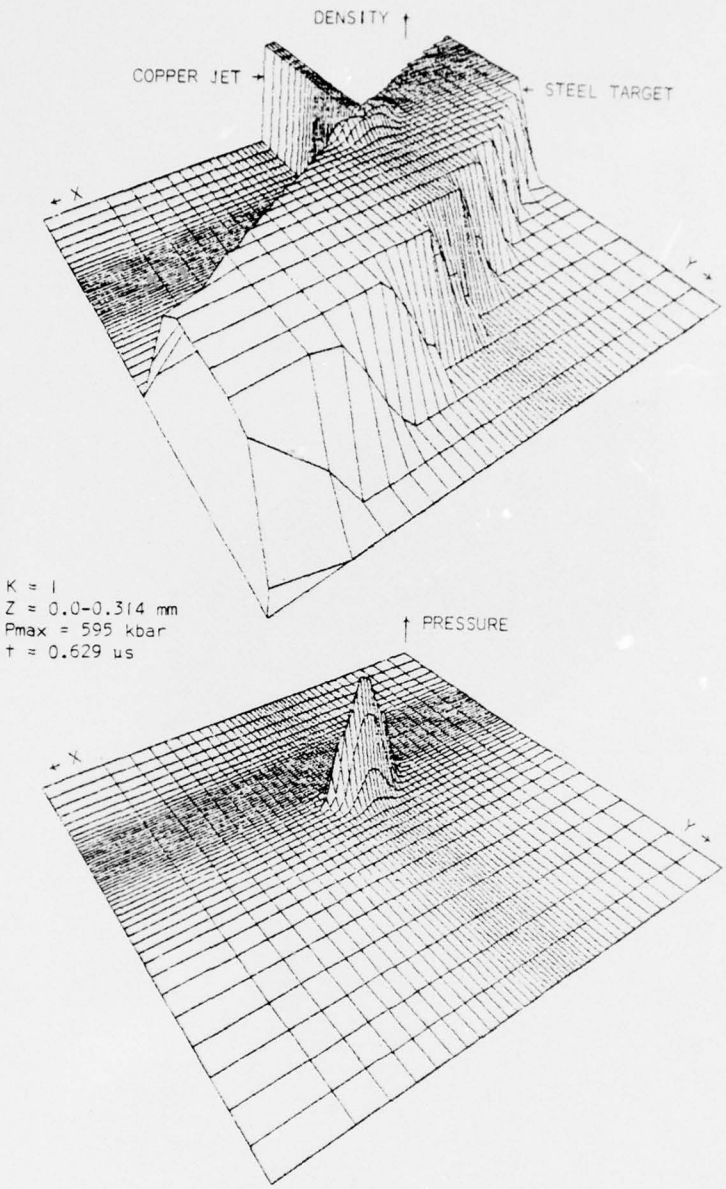

Figure 4. Density and Pressure Fields

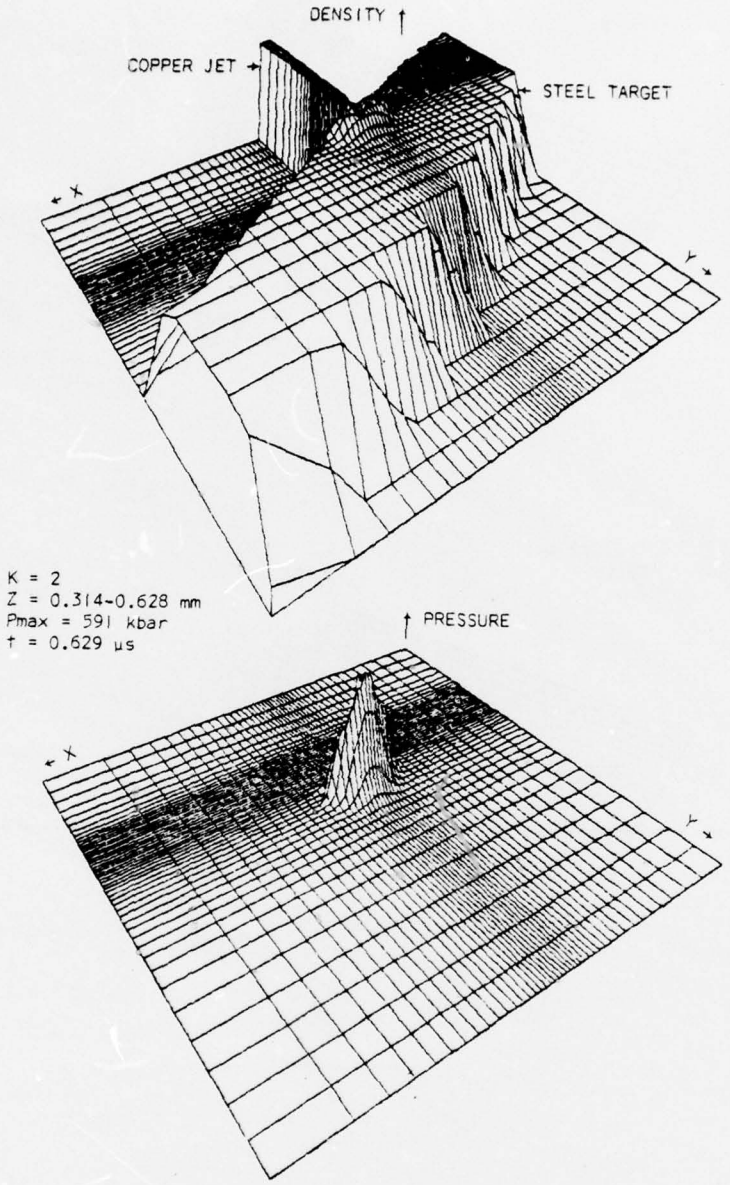

Figure 5. Density and Pressure Fields

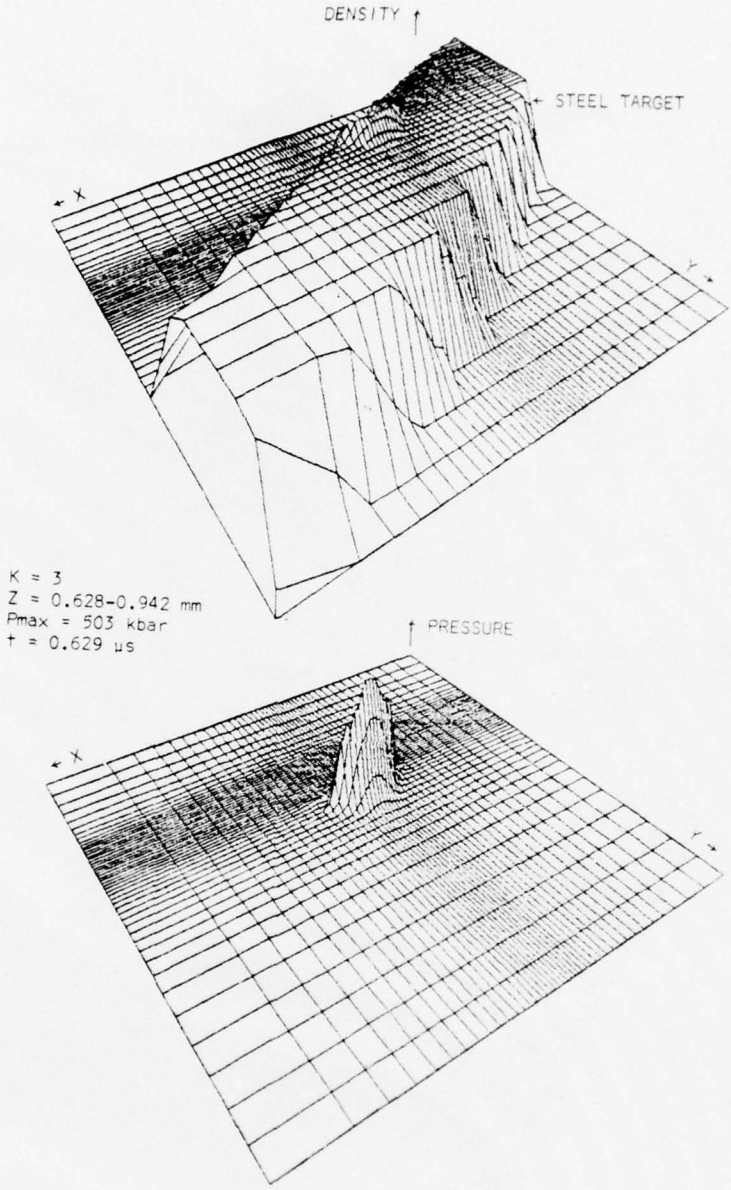

Figure 6. Density and Pressure Fields

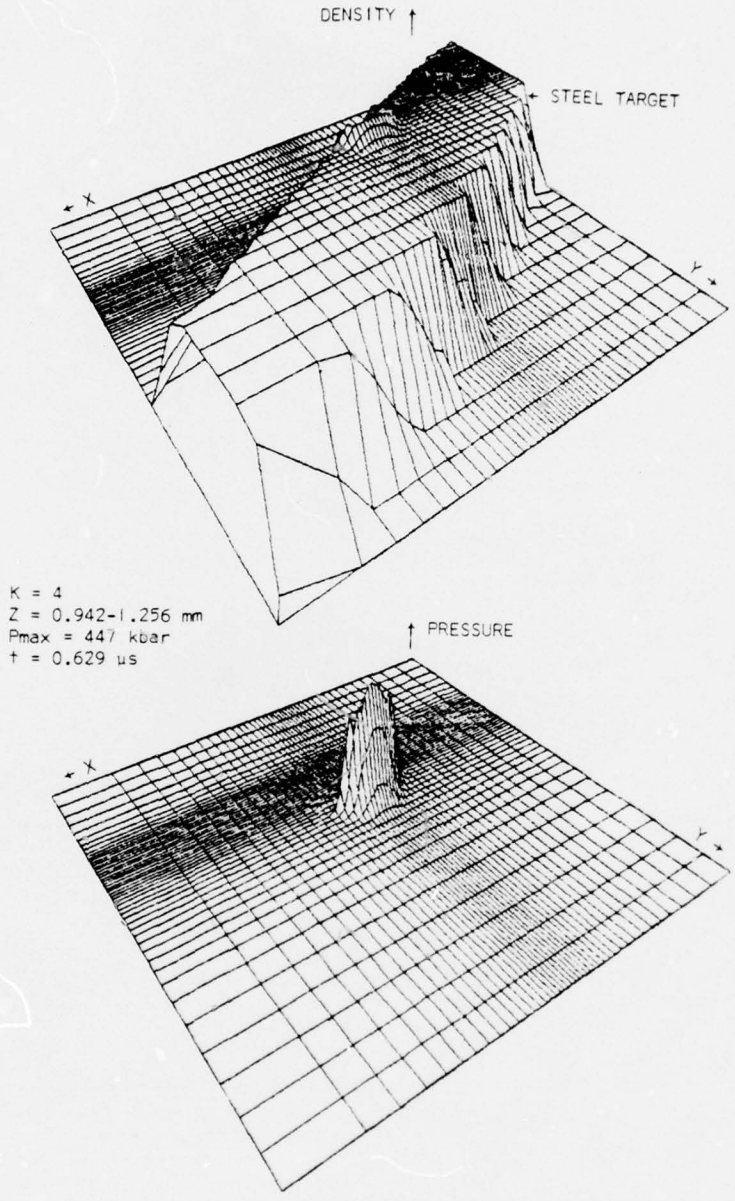

Figure 7. Density and Pressure Fields

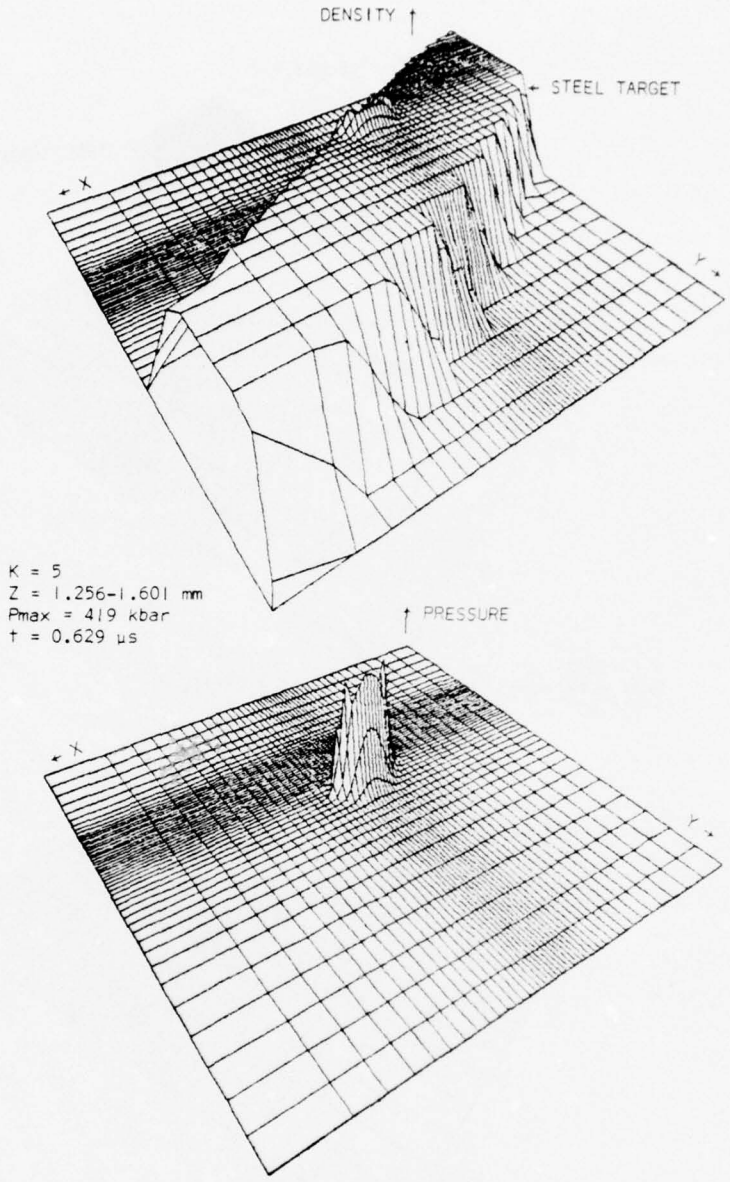

Figure 8. Density and Pressure Fields

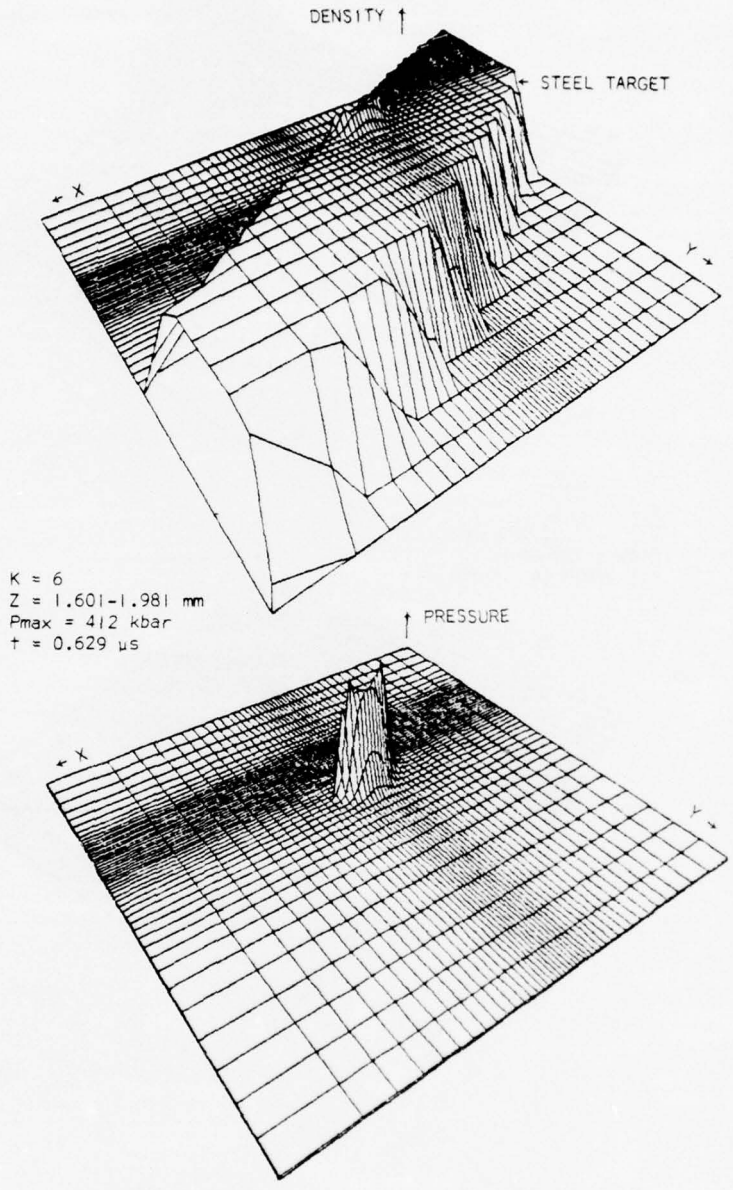

Figure 9. Density and Pressure Fields

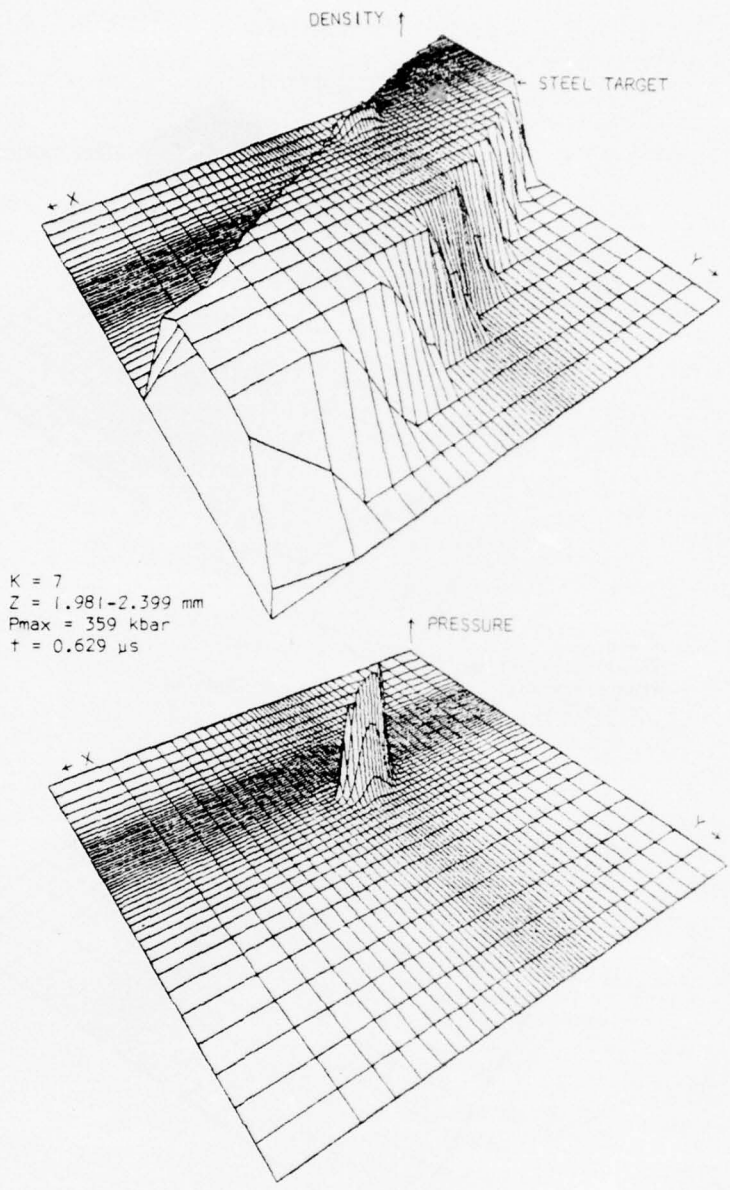

Figure 10. Density and Pressure Fields

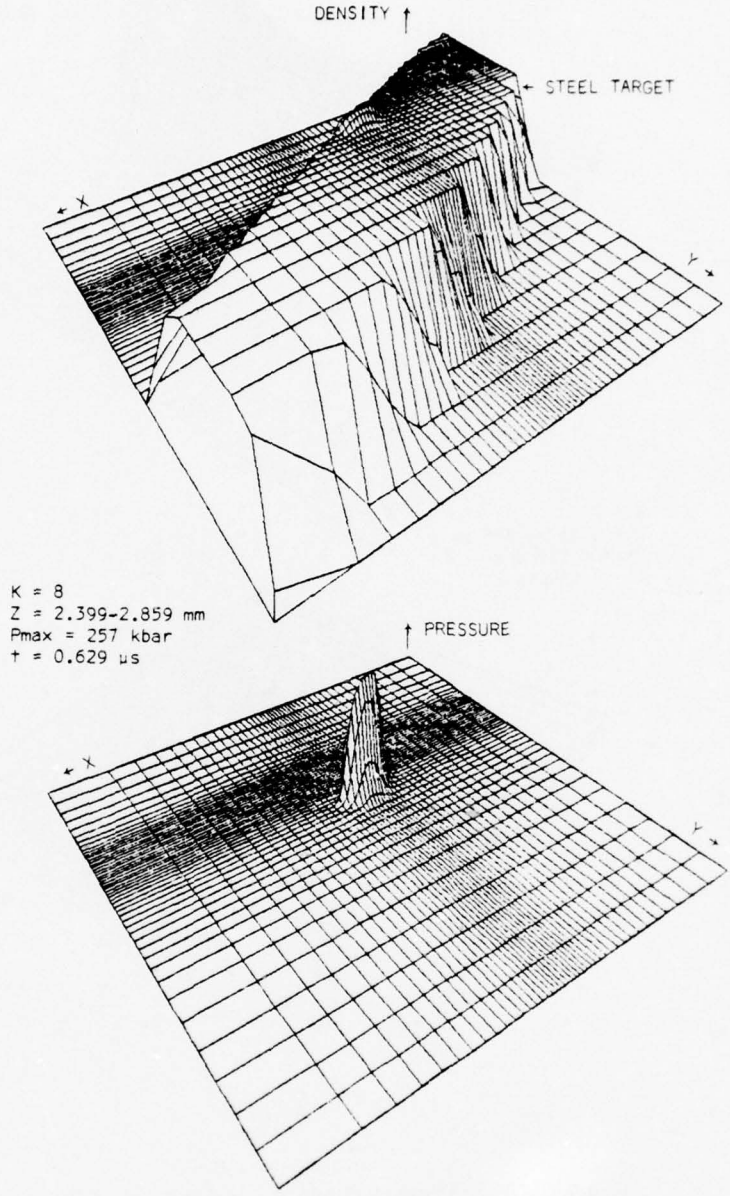

Figure 11. Density and Pressure Fields

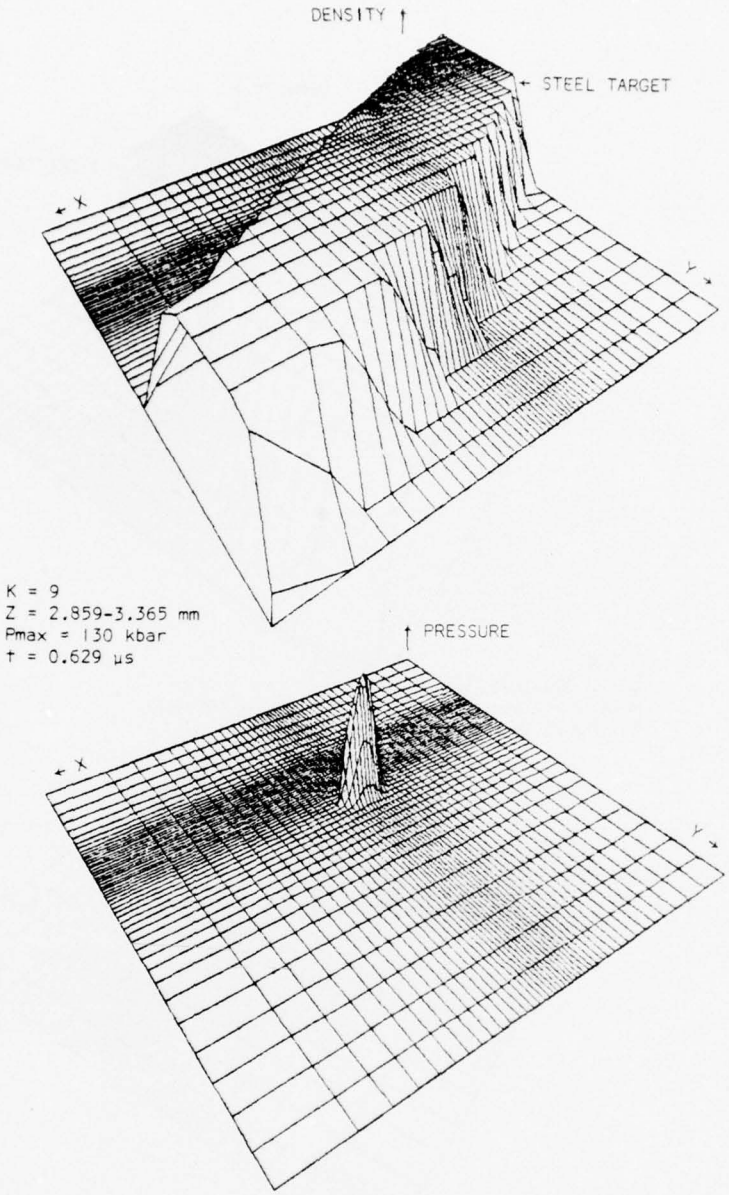

Figure 12. Density and Pressure Fields

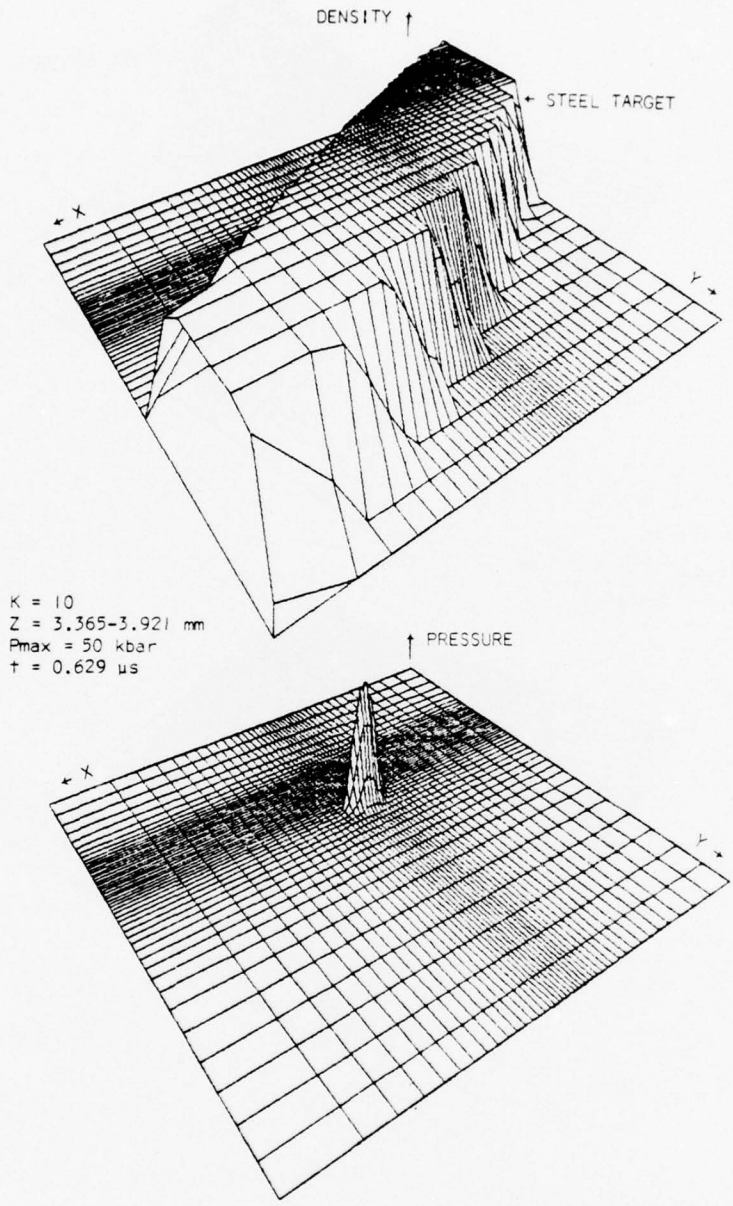

Figure 13. Density and Pressure Fields

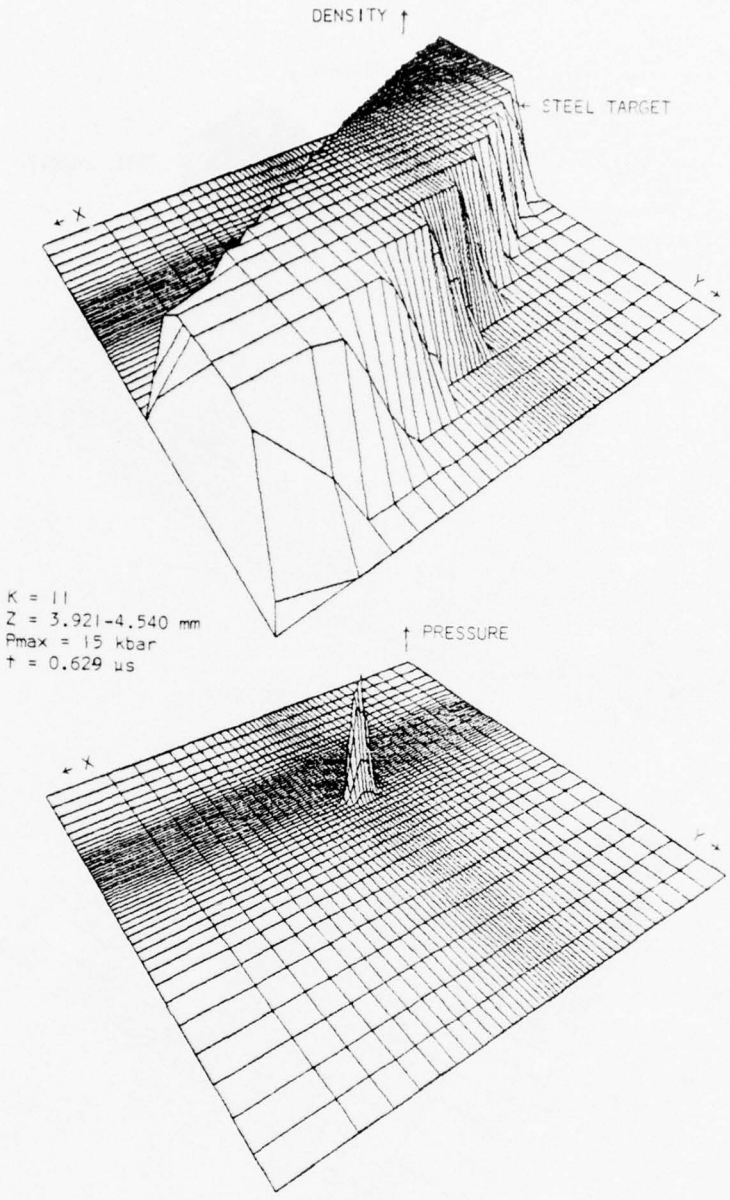

Figure 14. Density and Pressure Fields

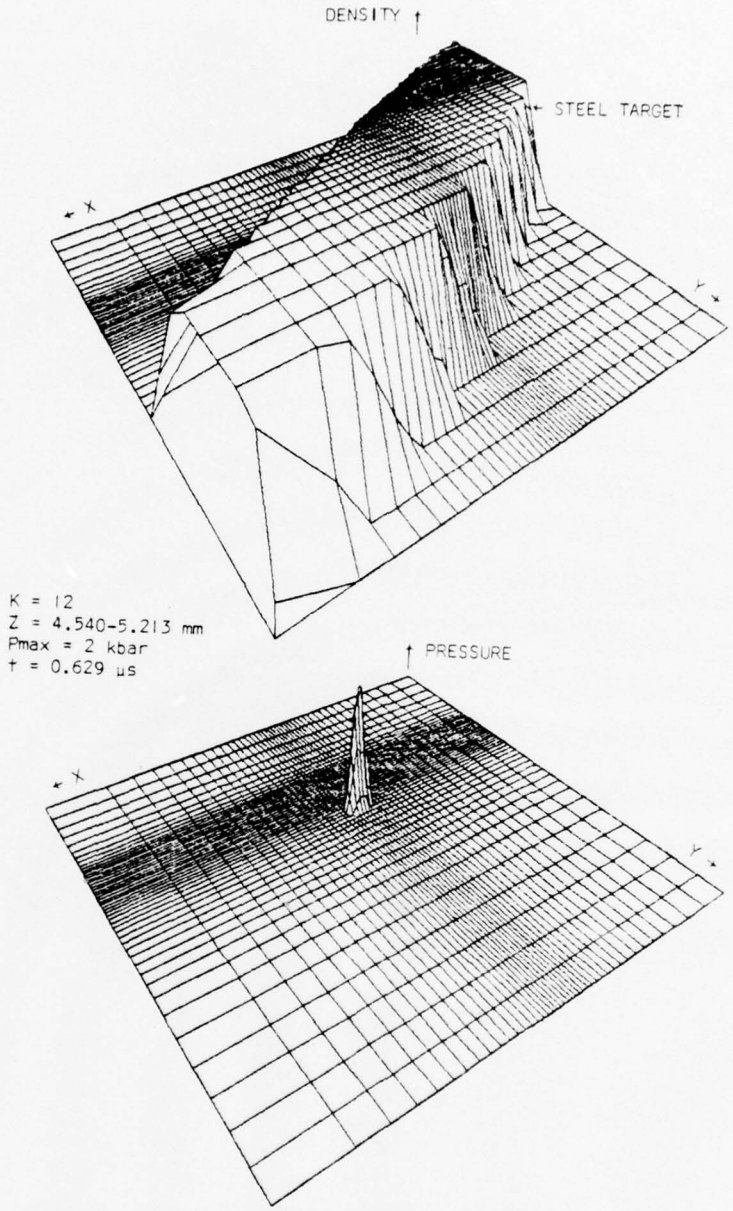

Figure 15. Density and Pressure Fields

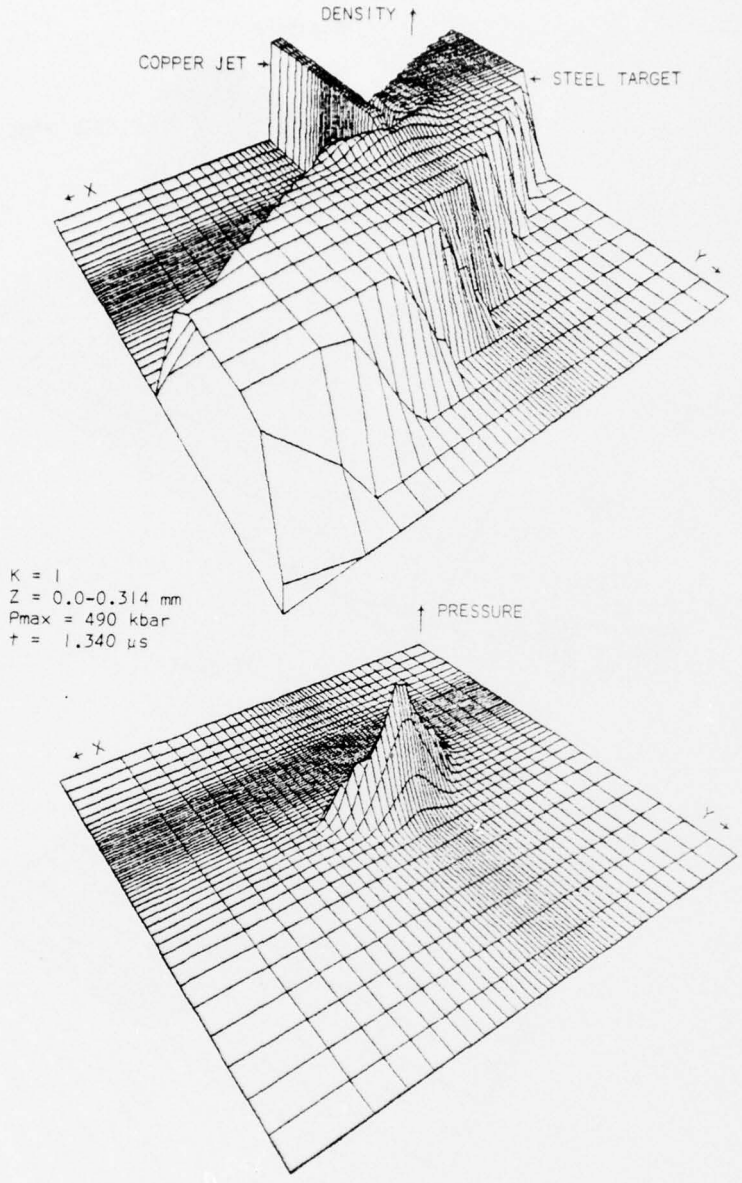

Figure 16. Density and Pressure Fields

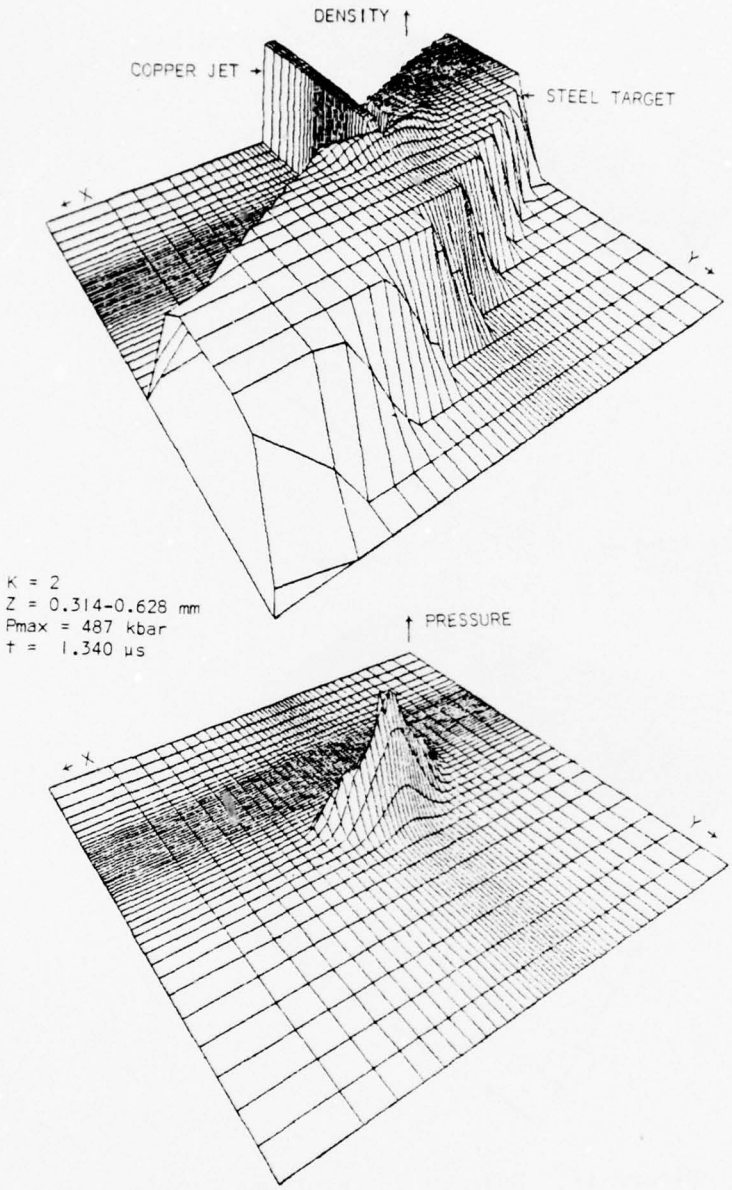

Figure 17. Density and Pressure Fields

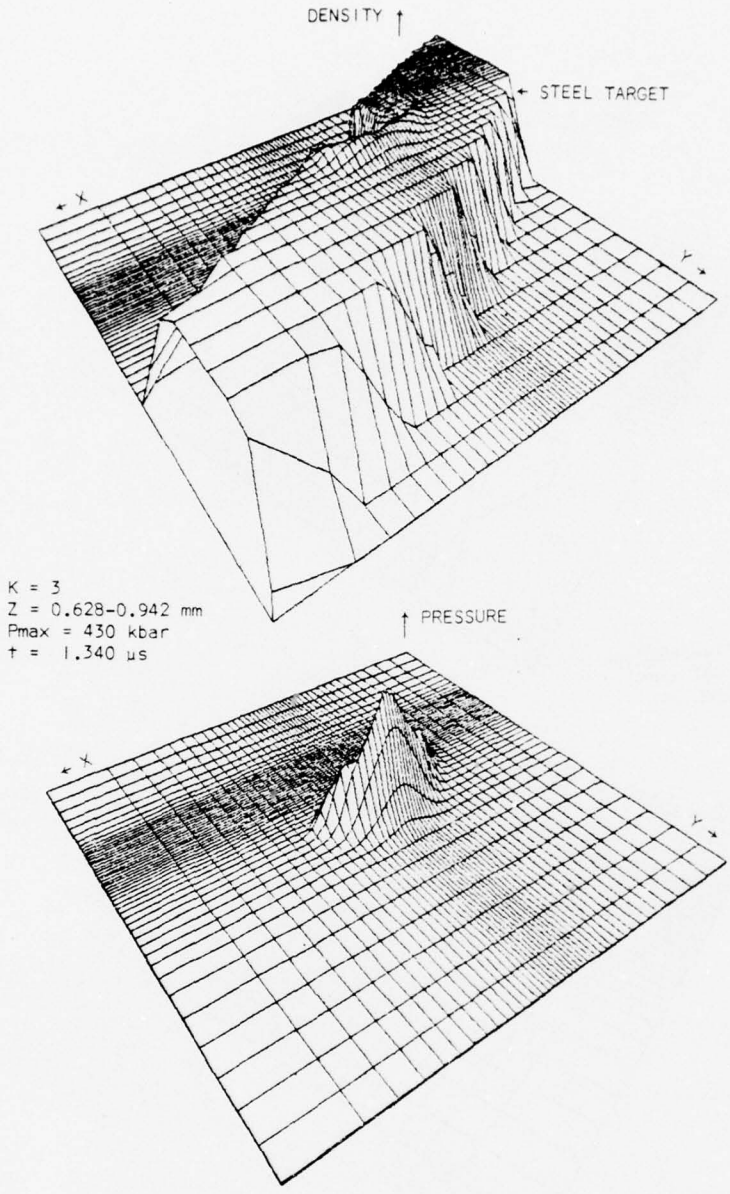

Figure 18. Density and Pressure Fields

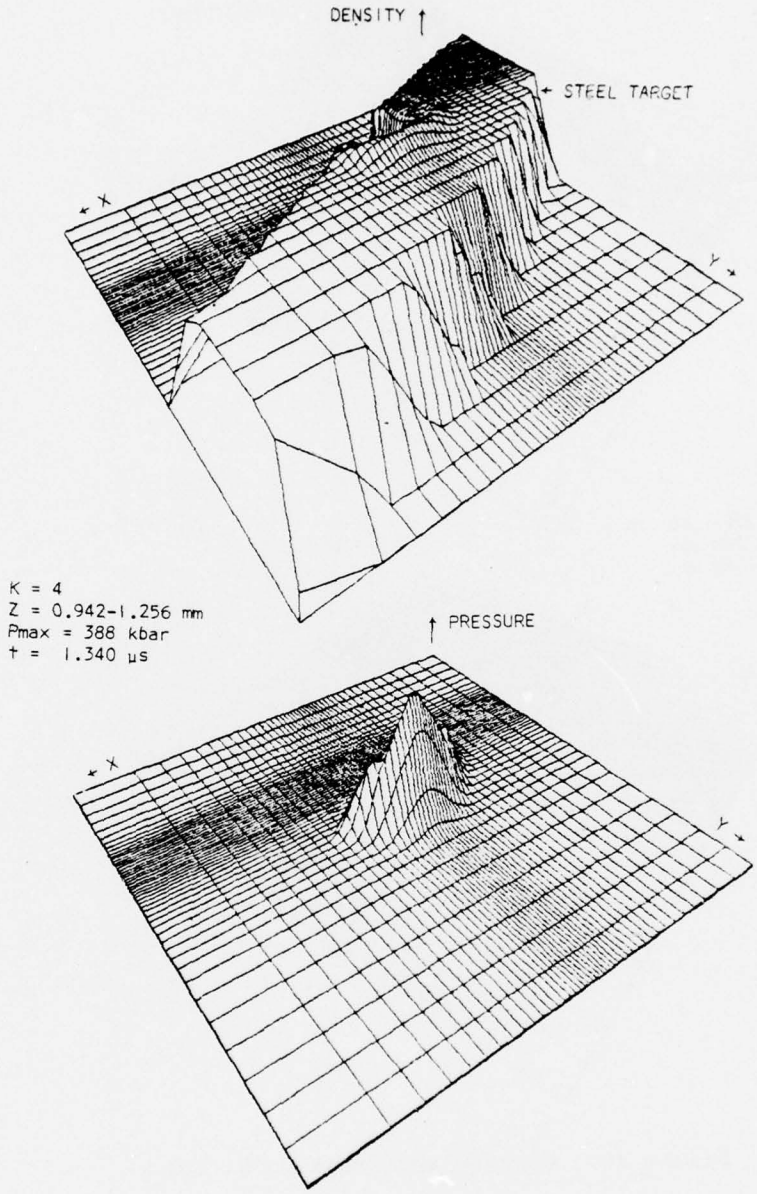

Figure 19. Density and Pressure Fields

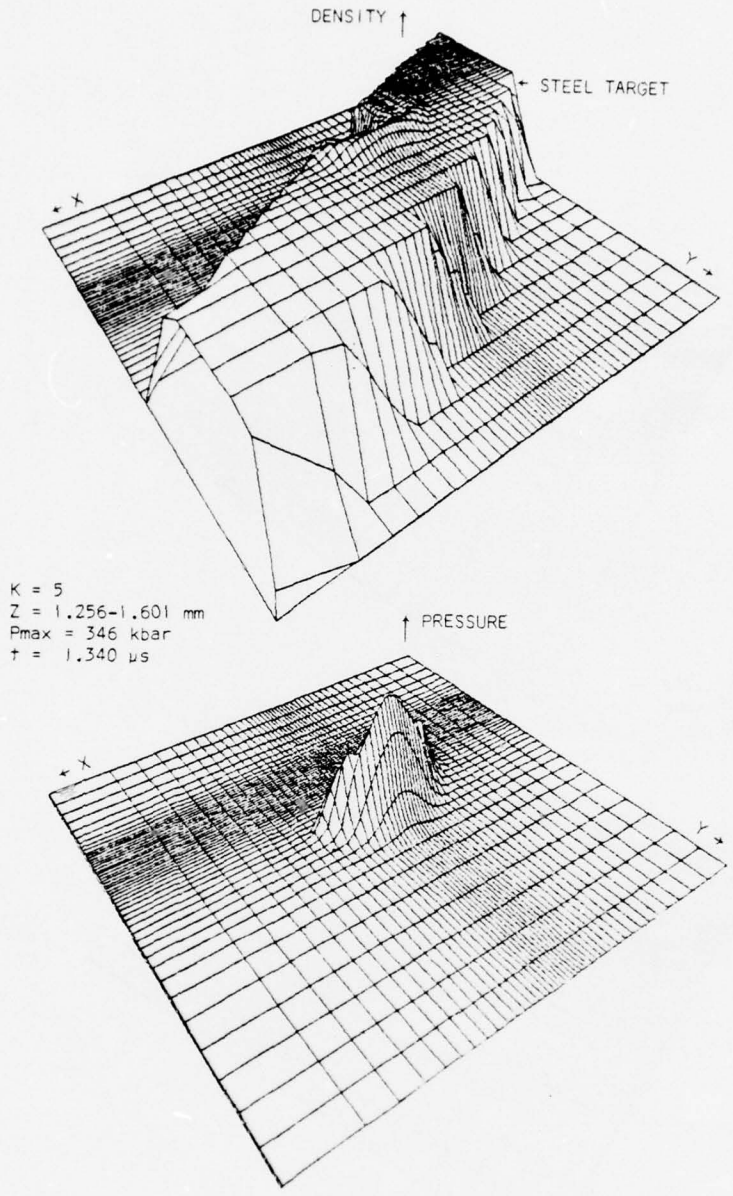

Figure 20. Density and Pressure Fields

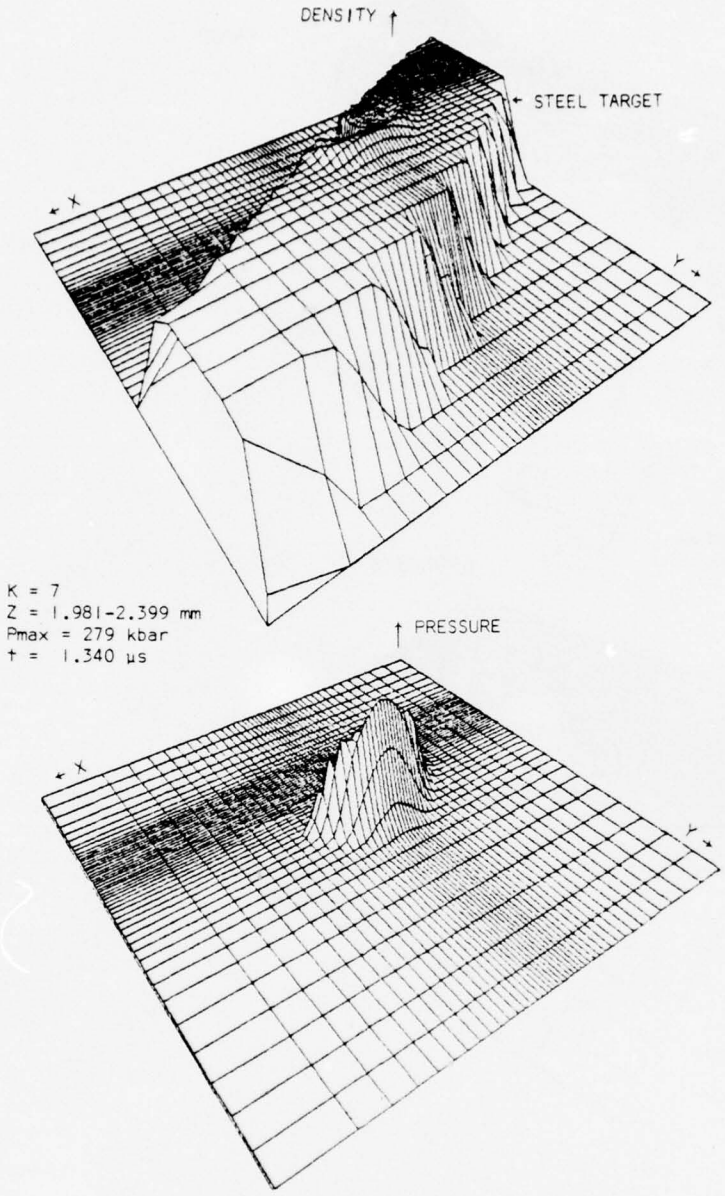

Figure 21. Density and Pressure Fields

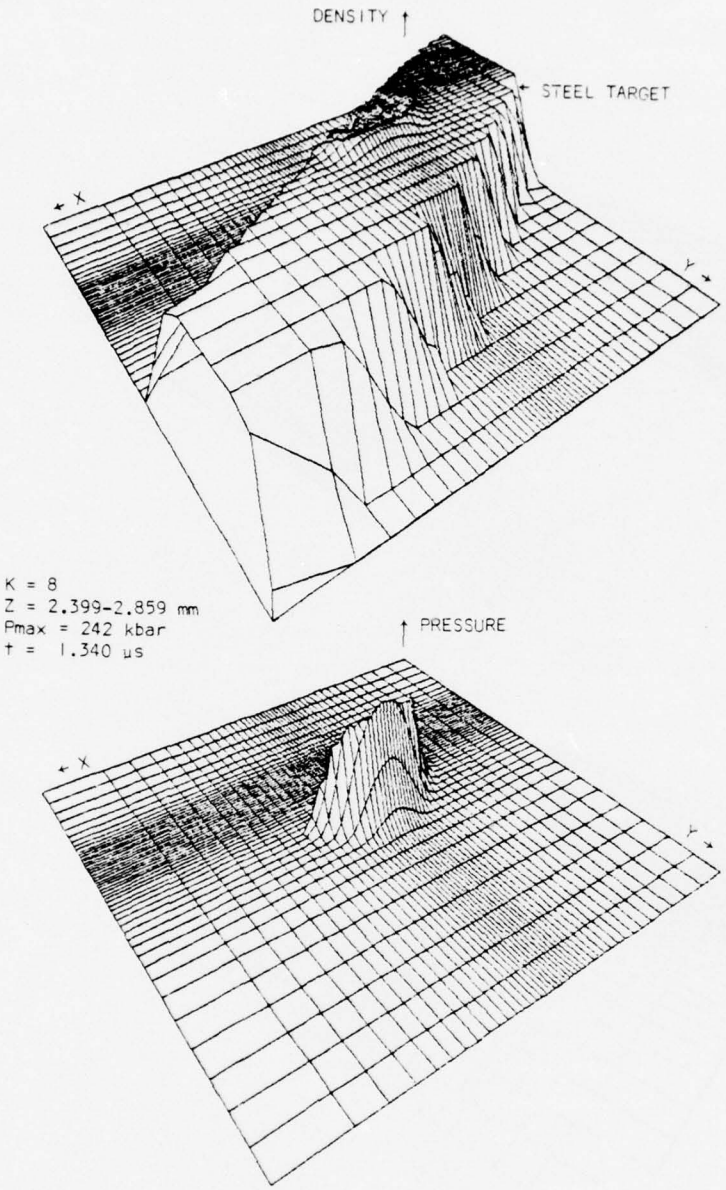

Figure 22. Density and Pressure Fields

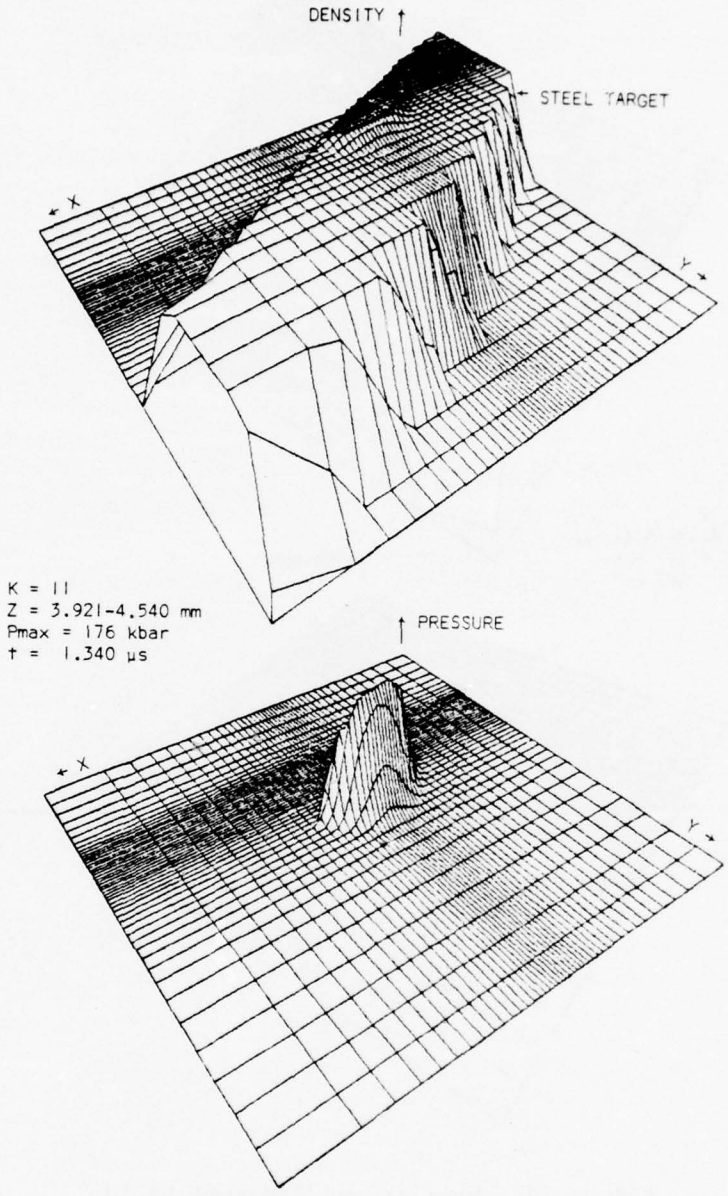

Figure 23. Density and Pressure Fields

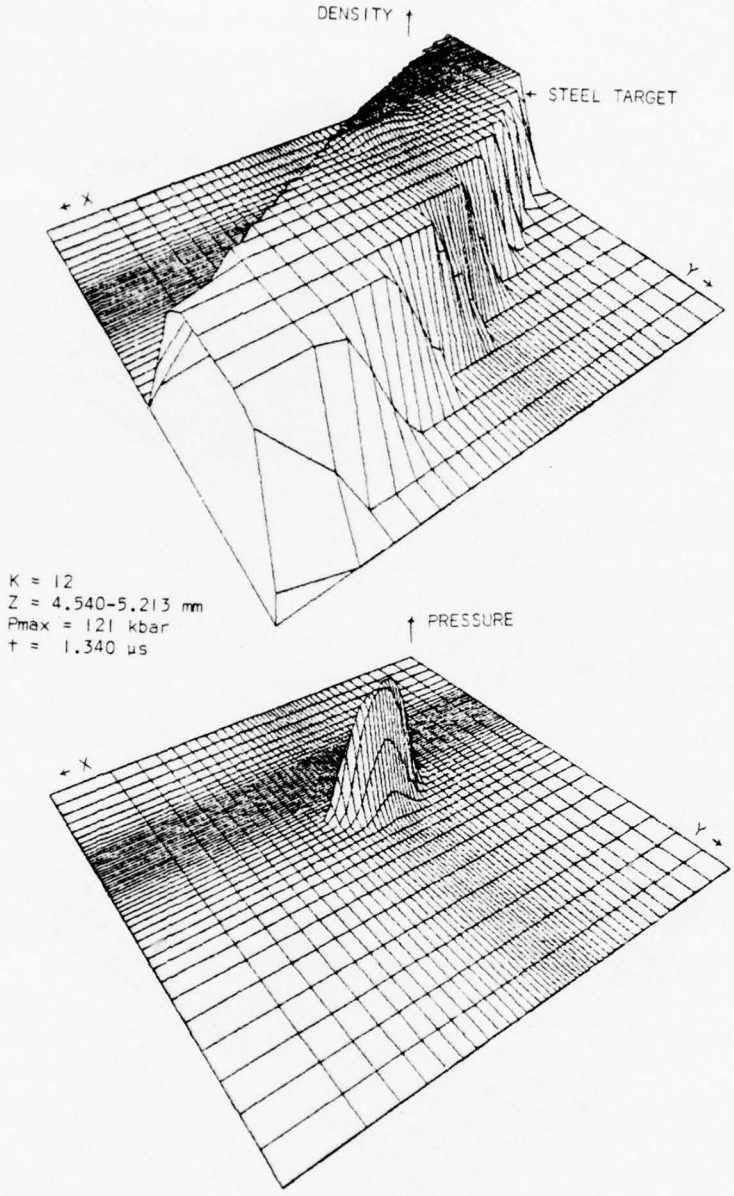

Figure 24. Density and Pressure Fields

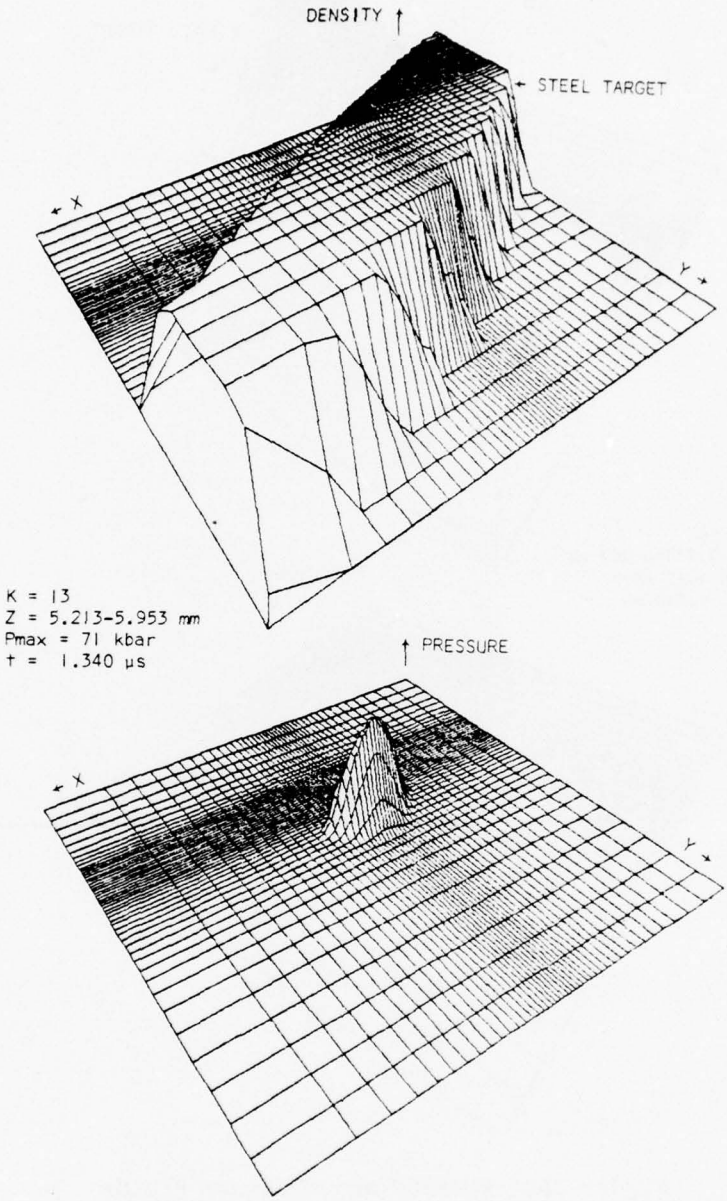

Figure 25. Density and Pressure Fields

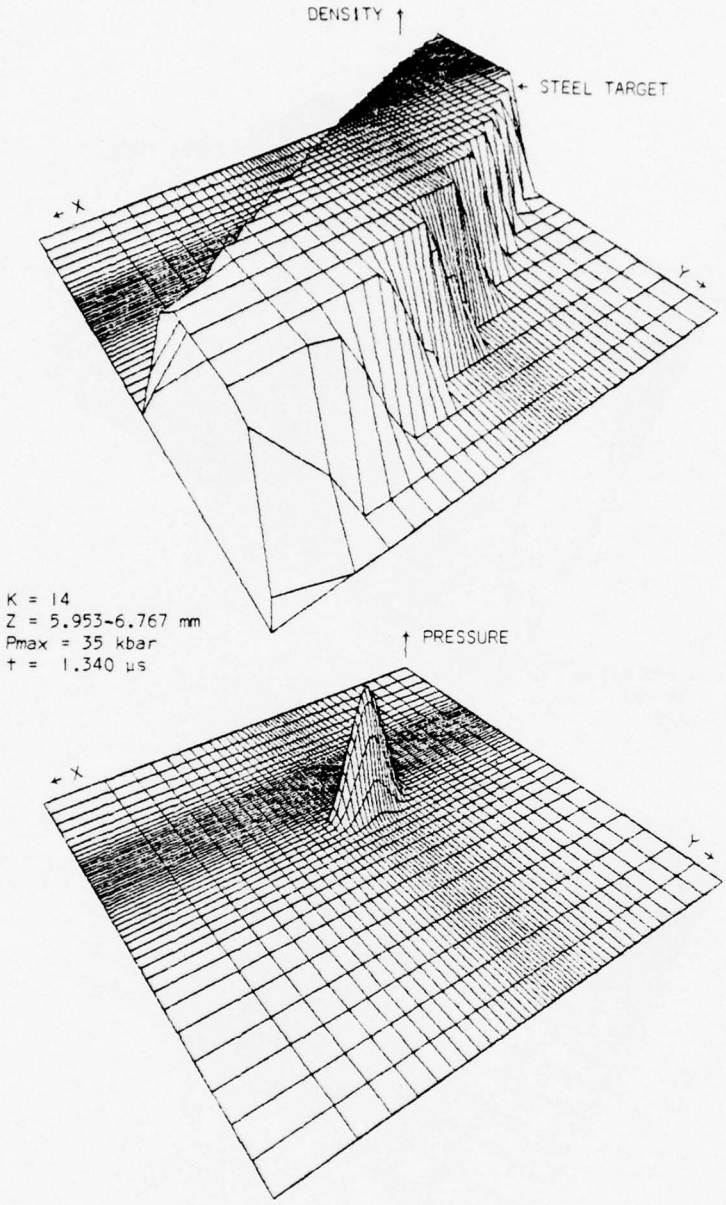

Figure 26. Density and Pressure Fields

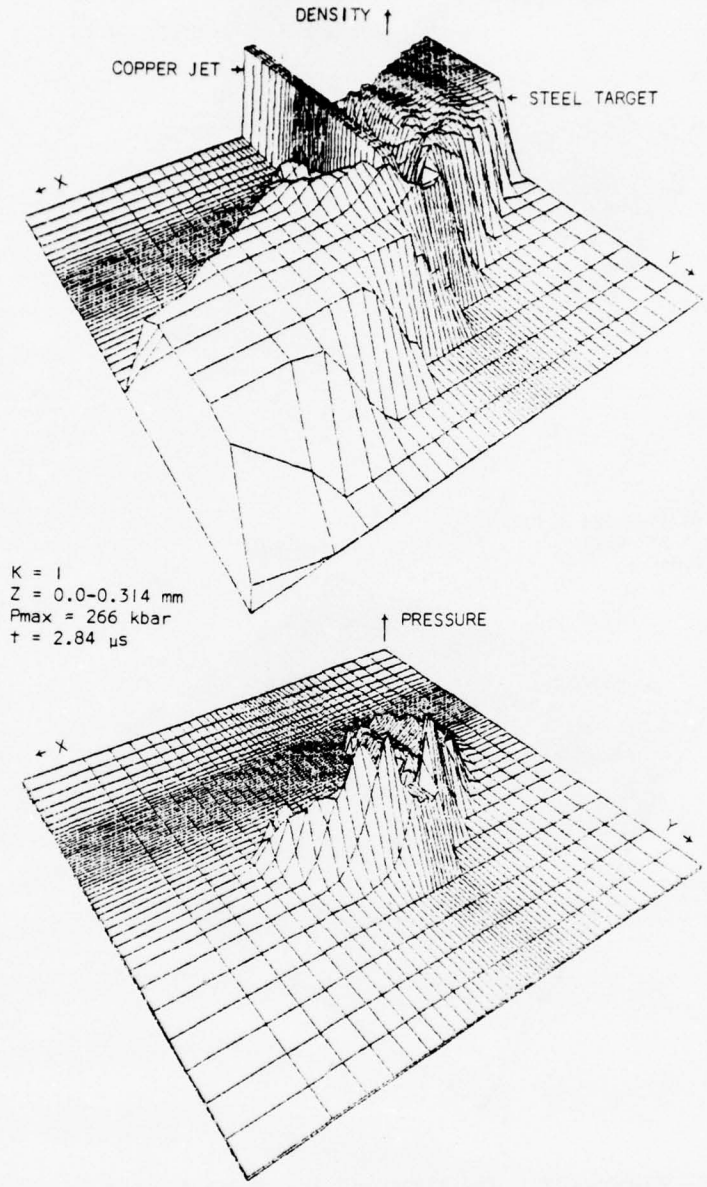

Figure 27. Density and Pressure Fields

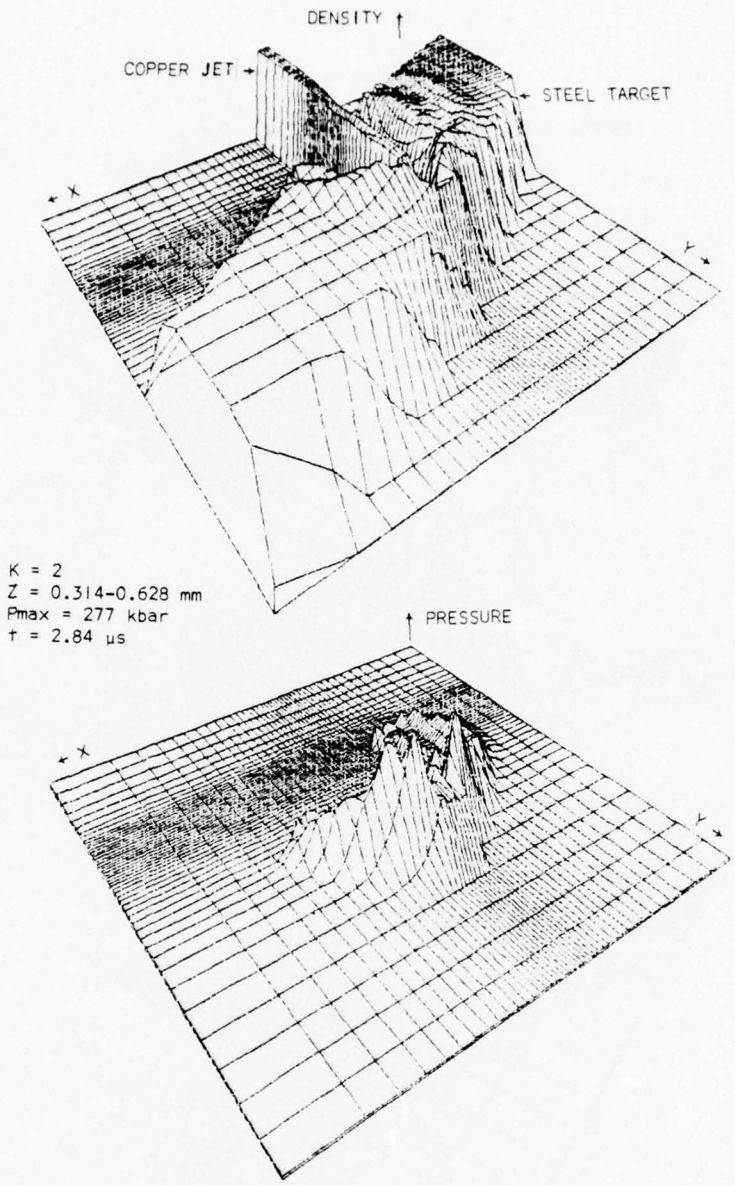

Figure 28. Density and Pressure Fields

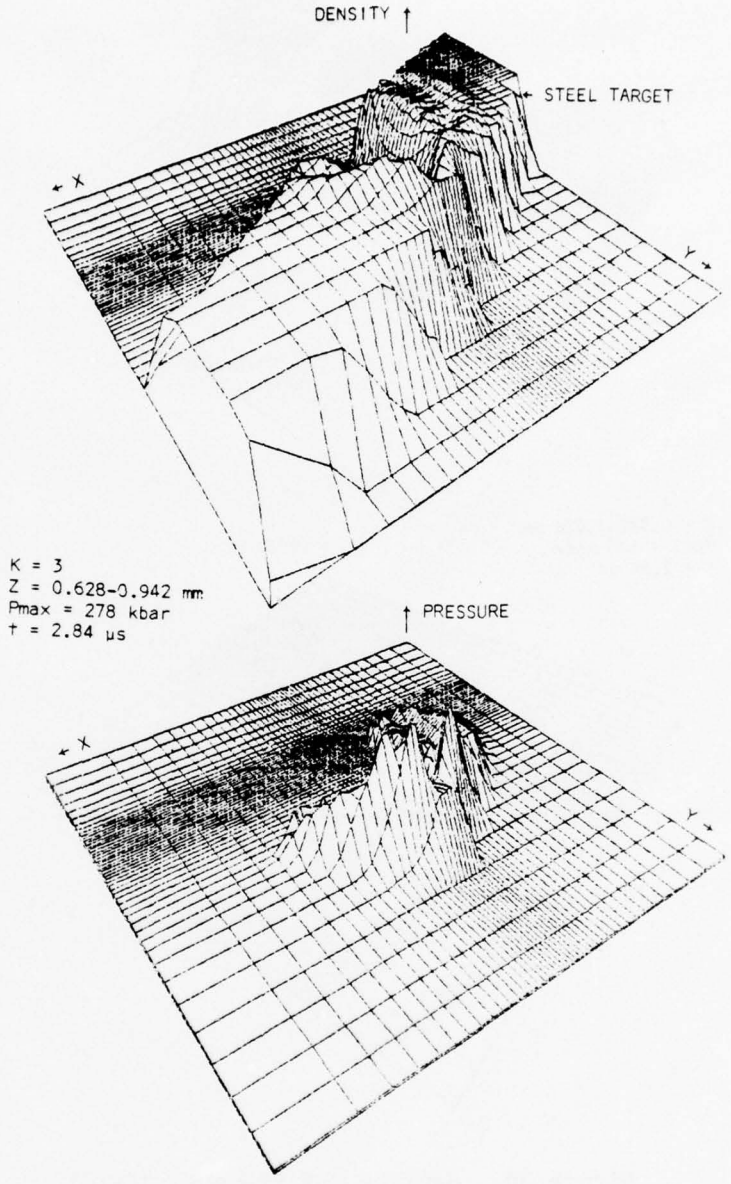

Figure 29. Density and Pressure Fields

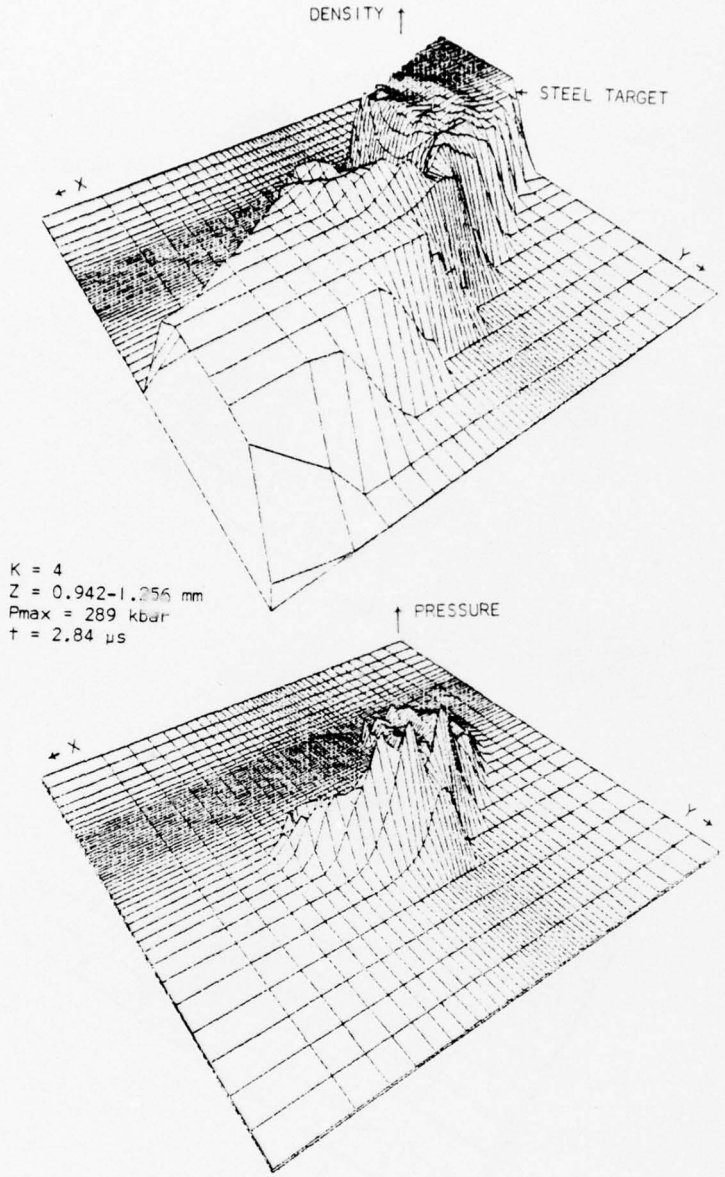

Figure 30. Density and Pressure Fields

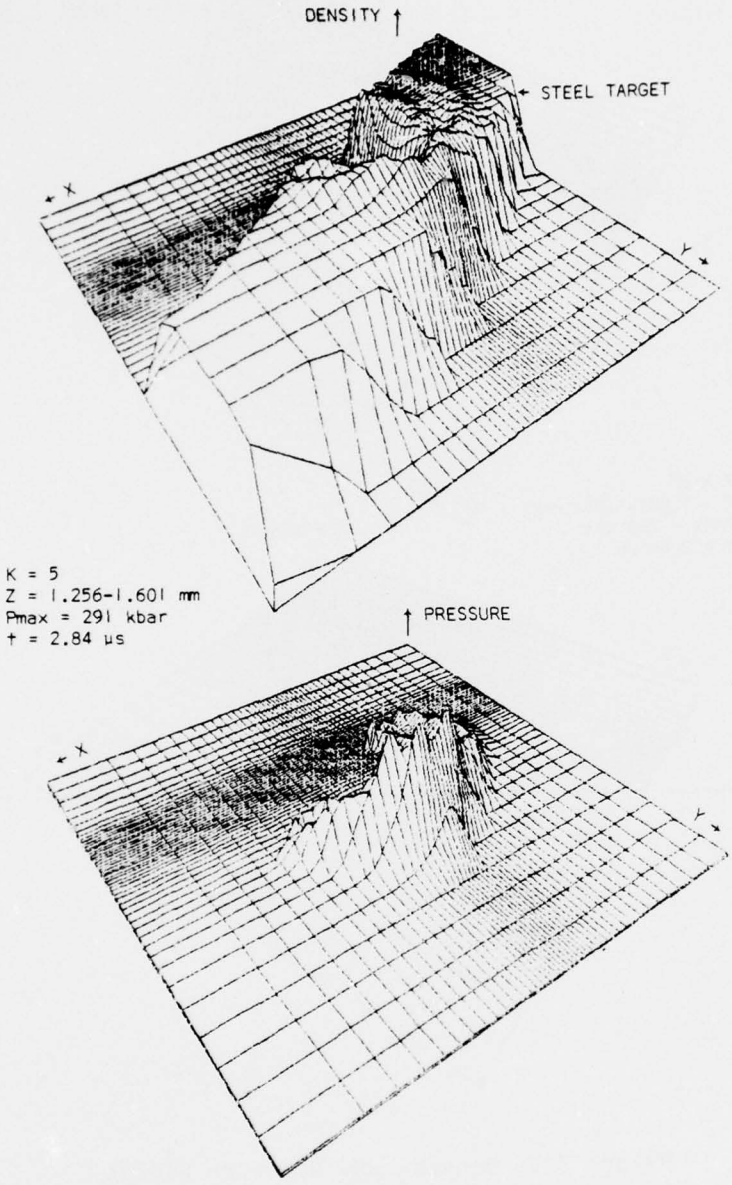

Figure 31. Density and Pressure Fields

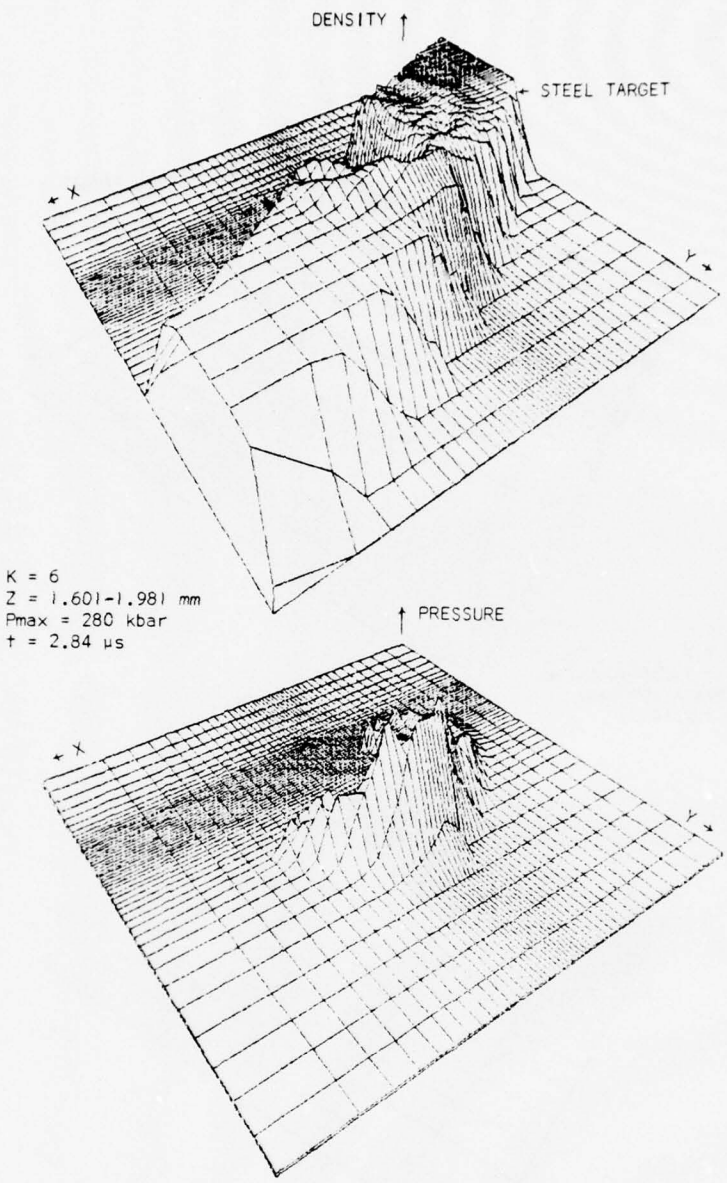

Figure 32. Density and Pressure Fields

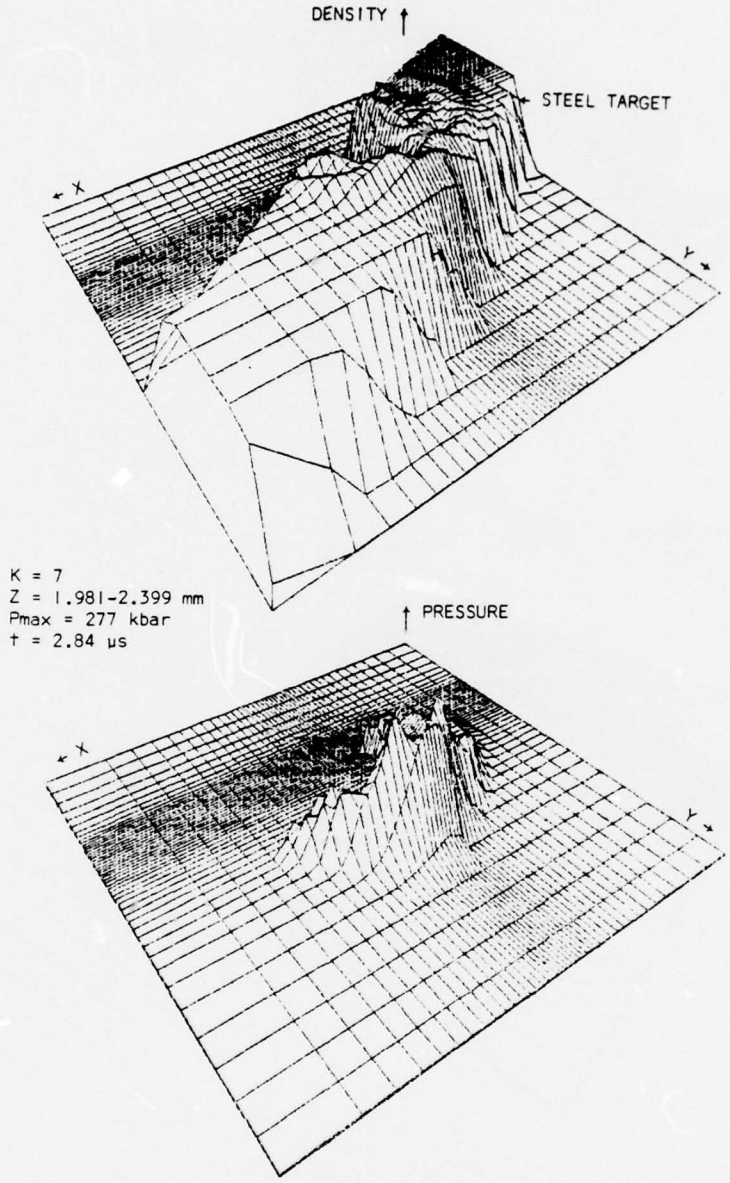

Figure 33. Density and Pressure Fields

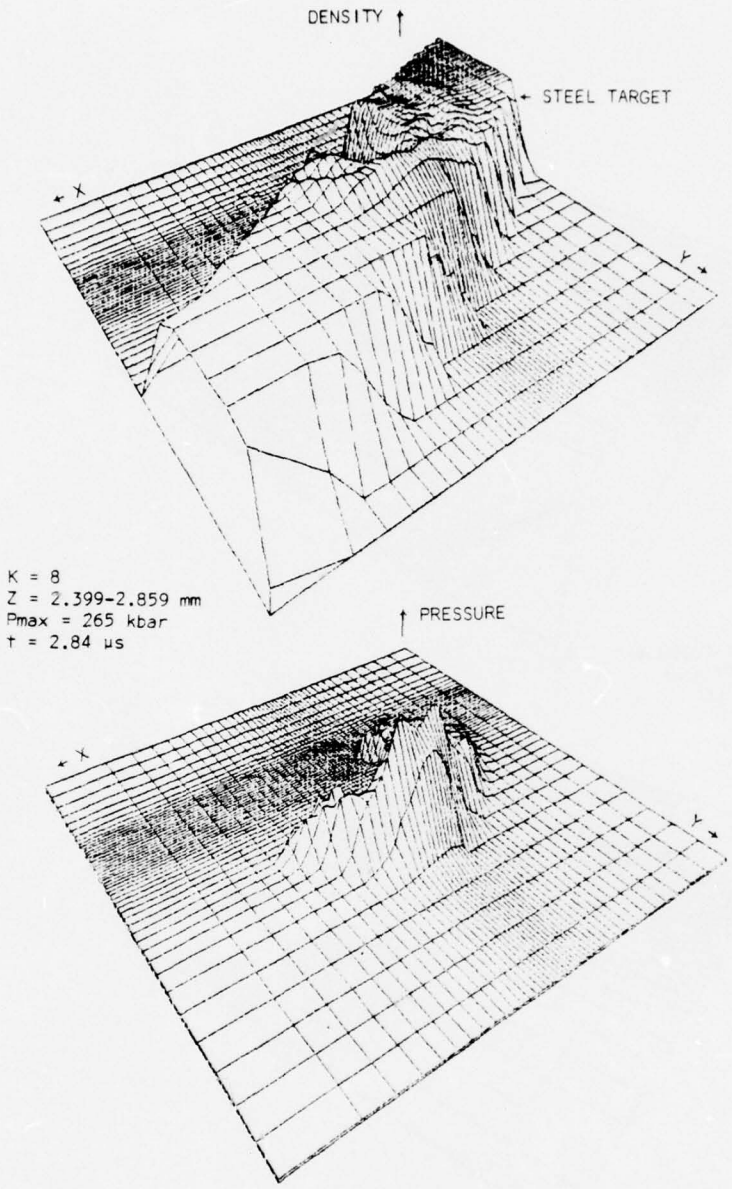

Figure 34. Density and Pressure Fields

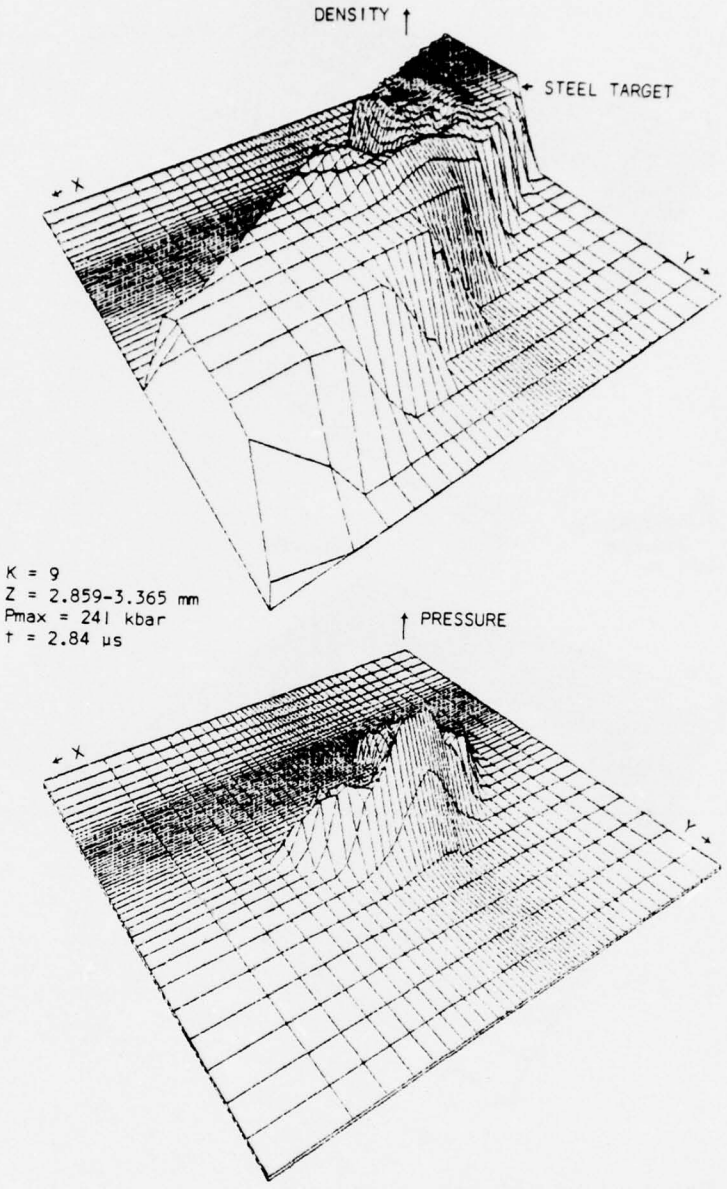

Figure 35. Density and Pressure Fields

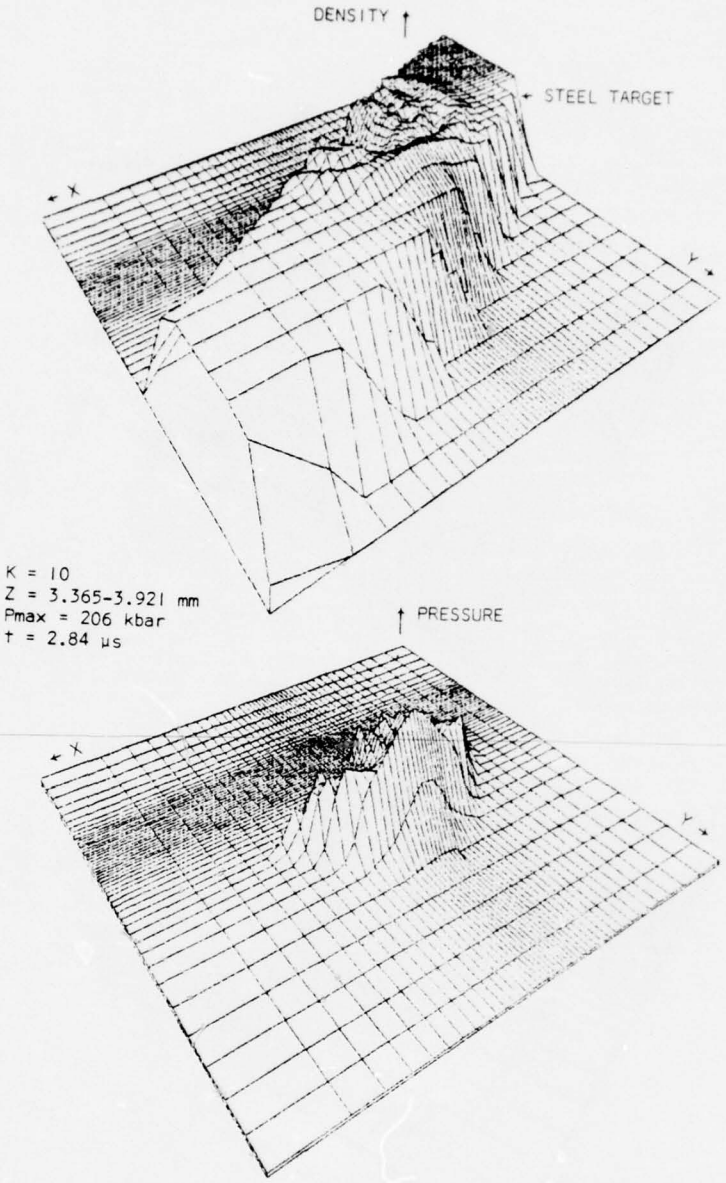

Figure 36. Density and Pressure Fields

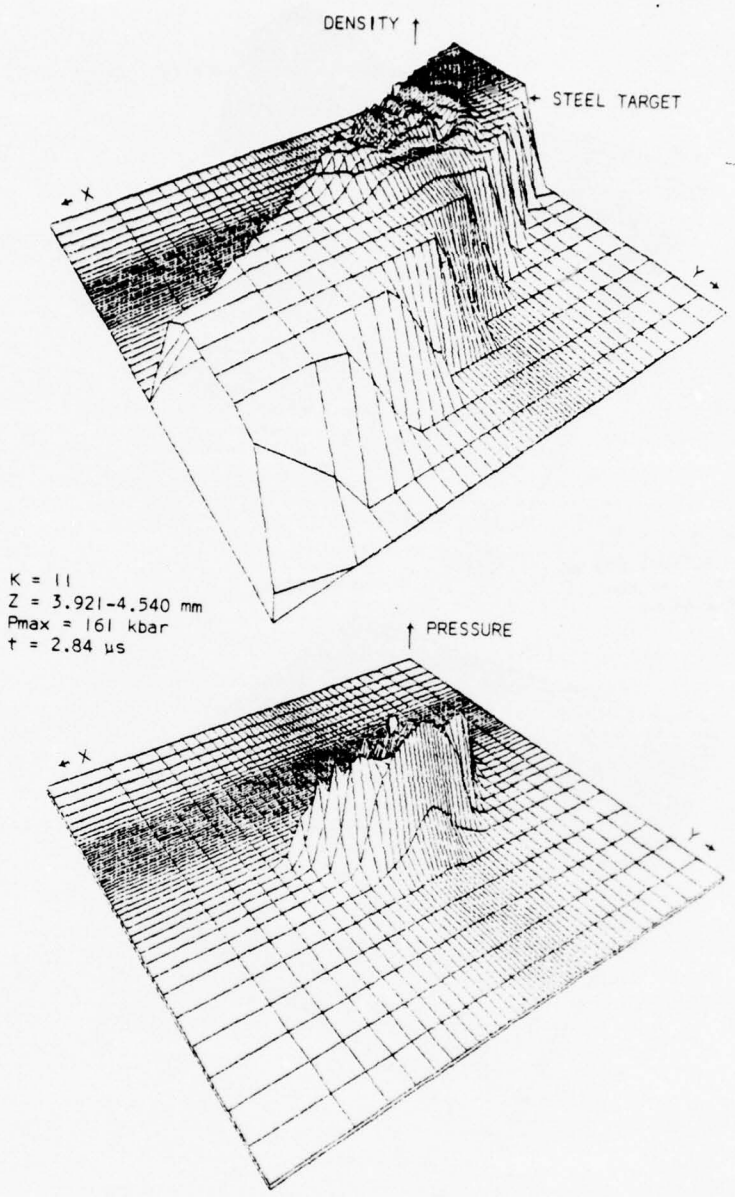

Figure 37. Density and Pressure Fields

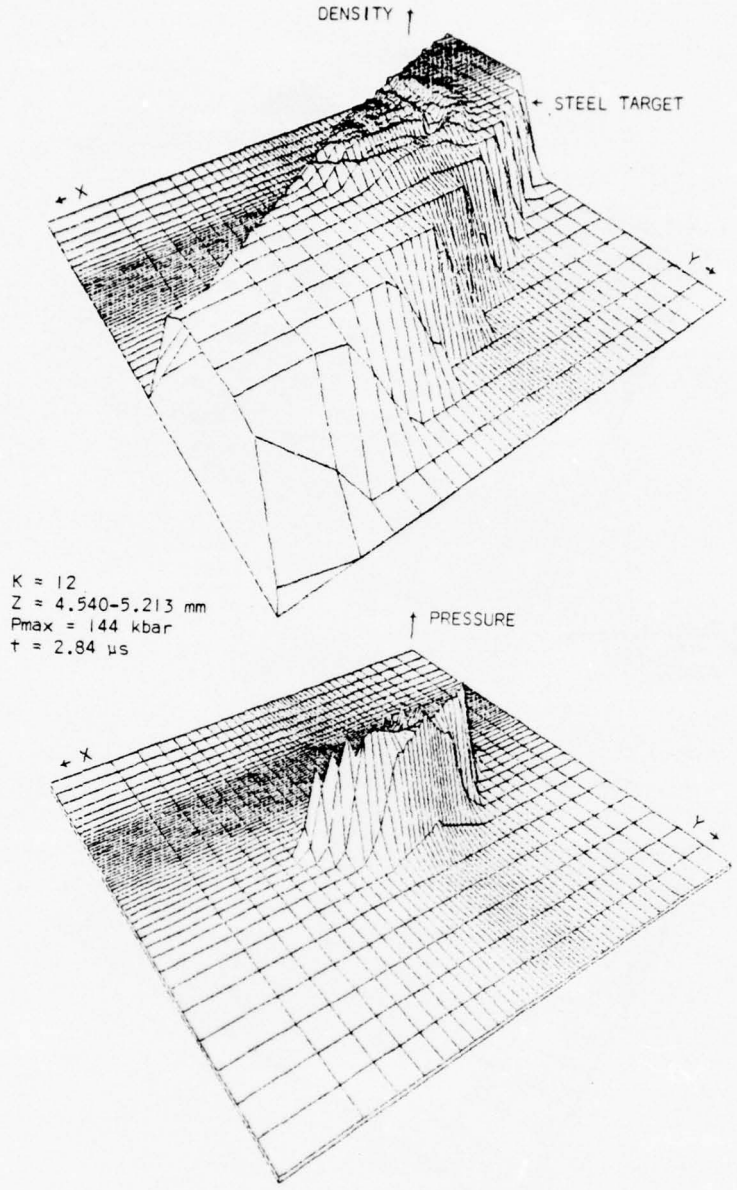

Figure 38. Density and Pressure Fields

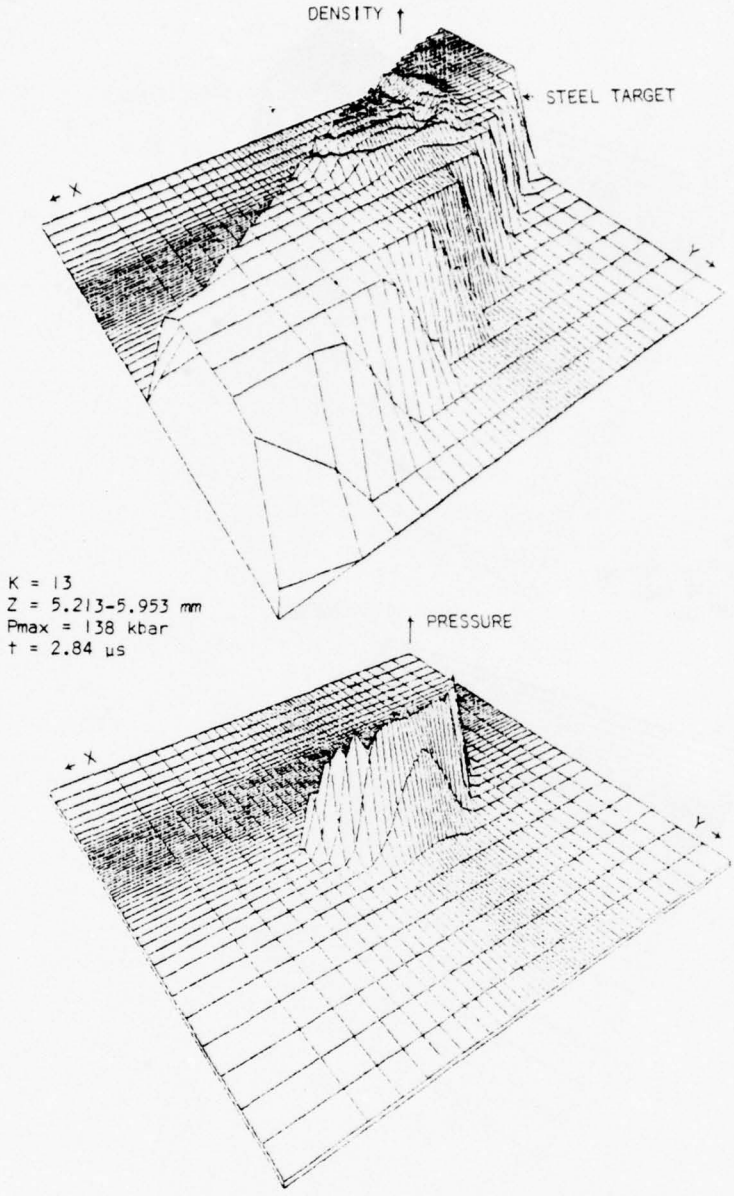

Figure 39. Density and Pressure Fields

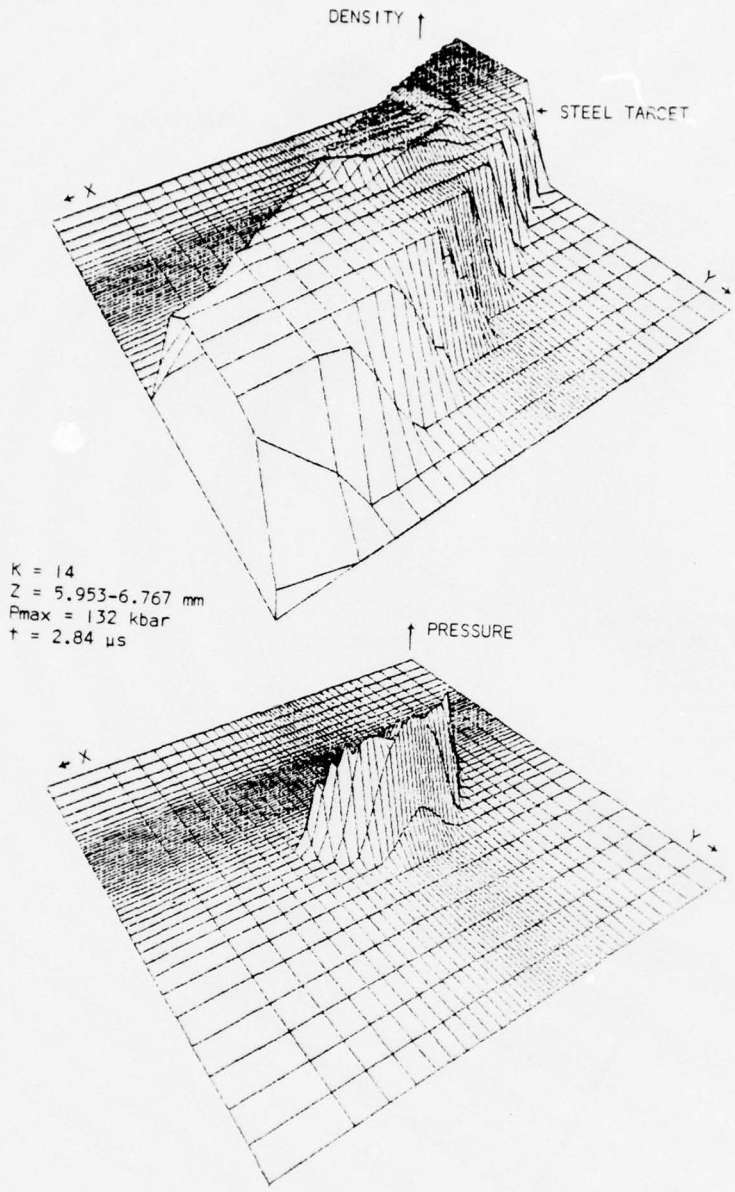

Figure 40. Density and Pressure Fields

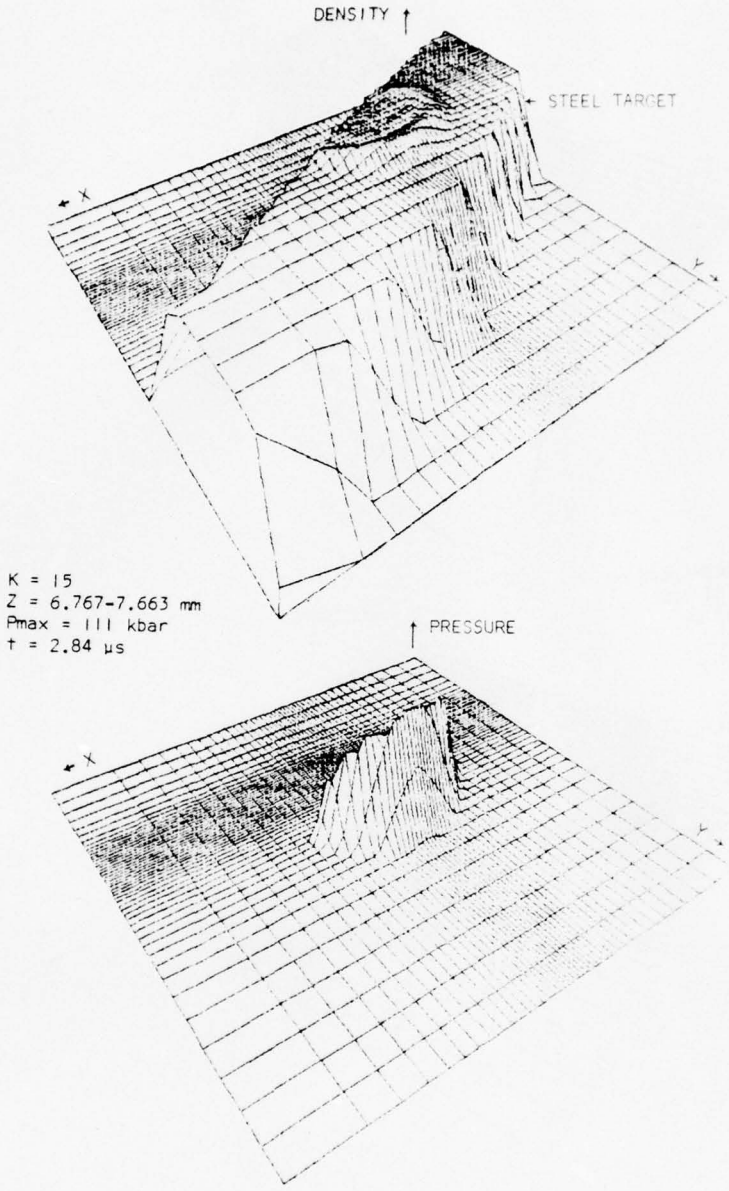

Figure 41. Density and Pressure Fields

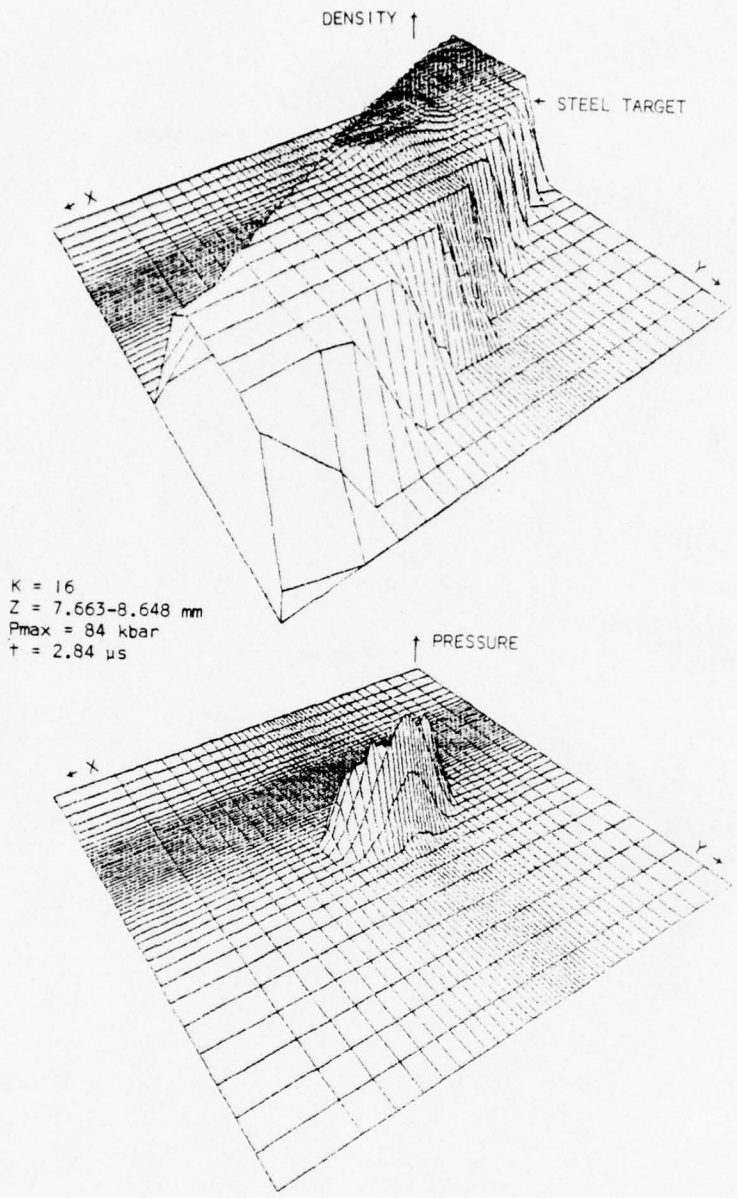

Figure 42. Density and Pressure Fields

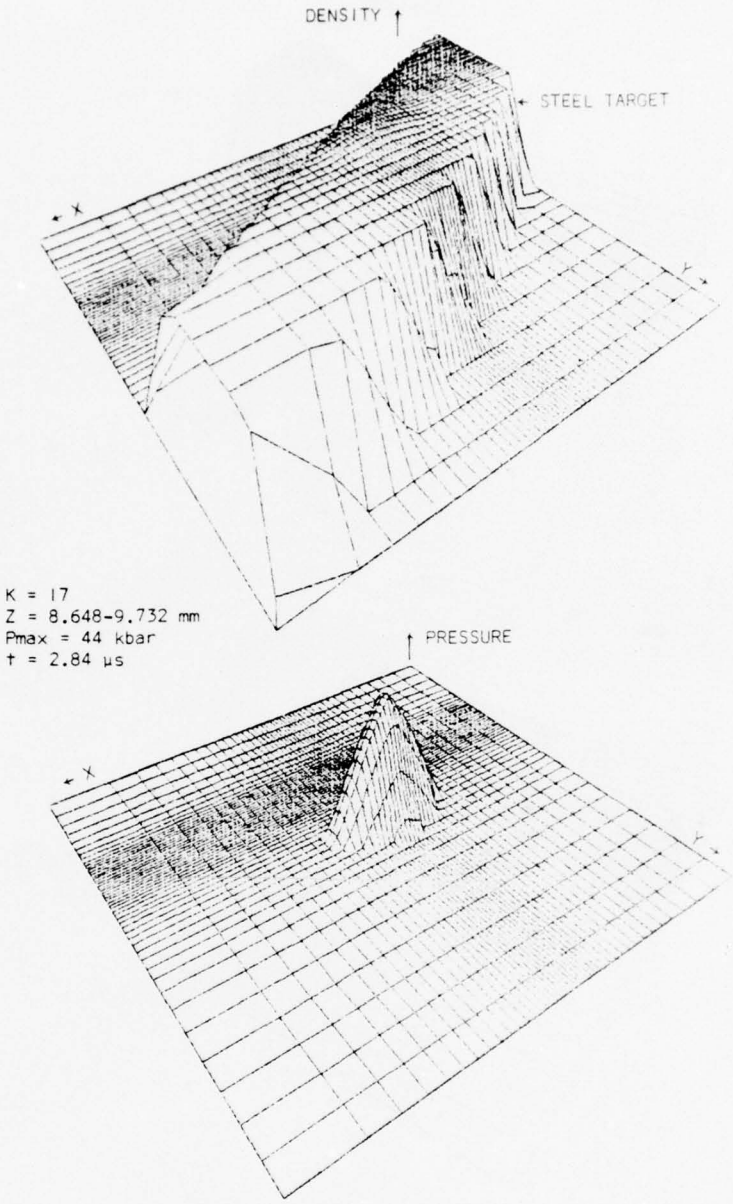

Figure 43. Density and Pressure Fields

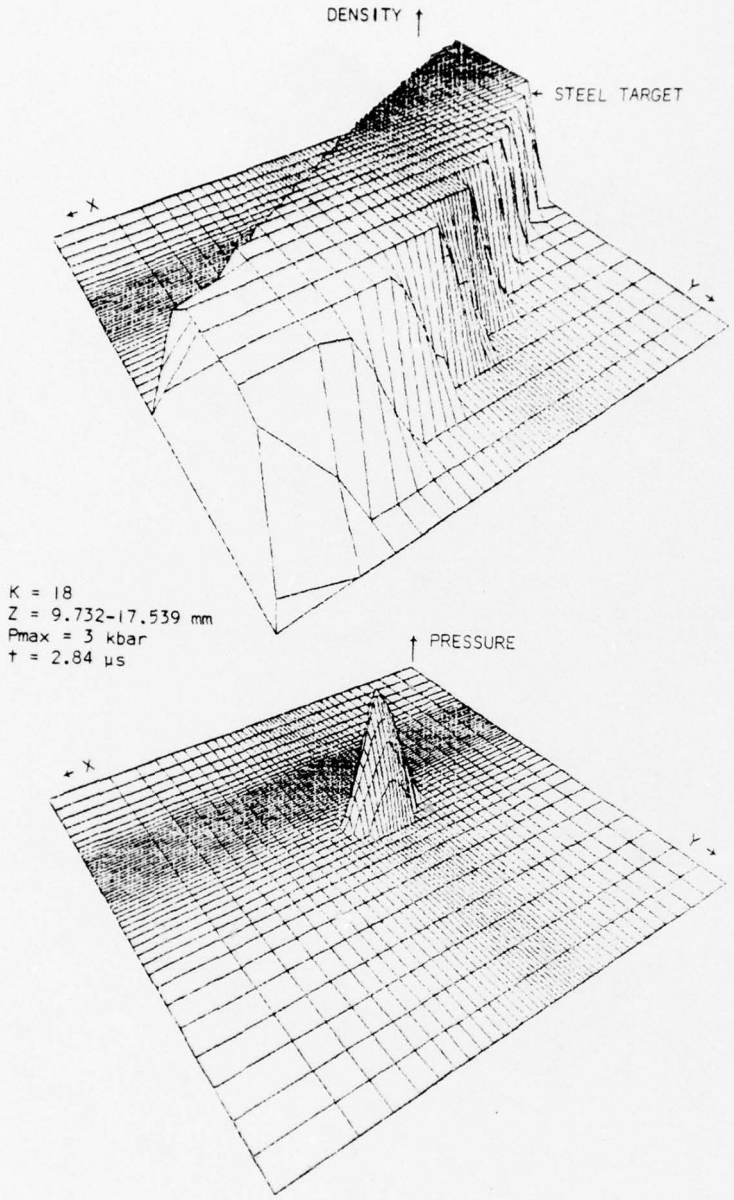

Figure 44. Density and Pressure Fields

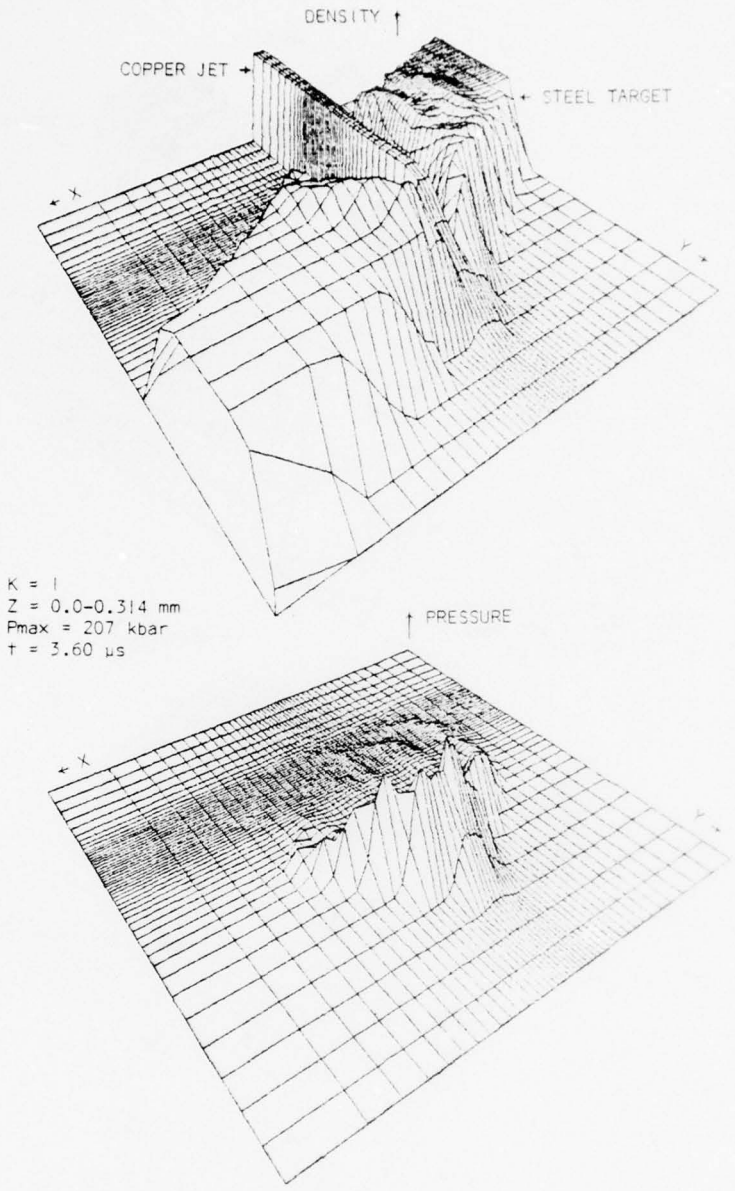

Figure 45. Density and Pressure Fields

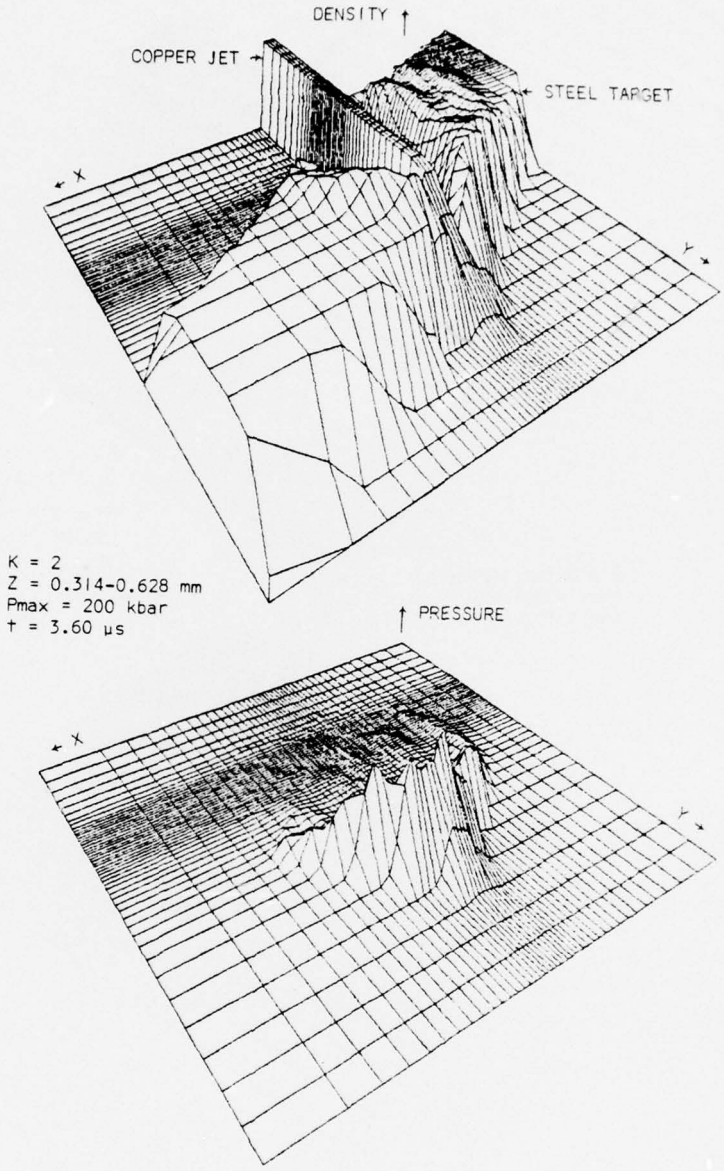

Figure 46. Density and Pressure Fields

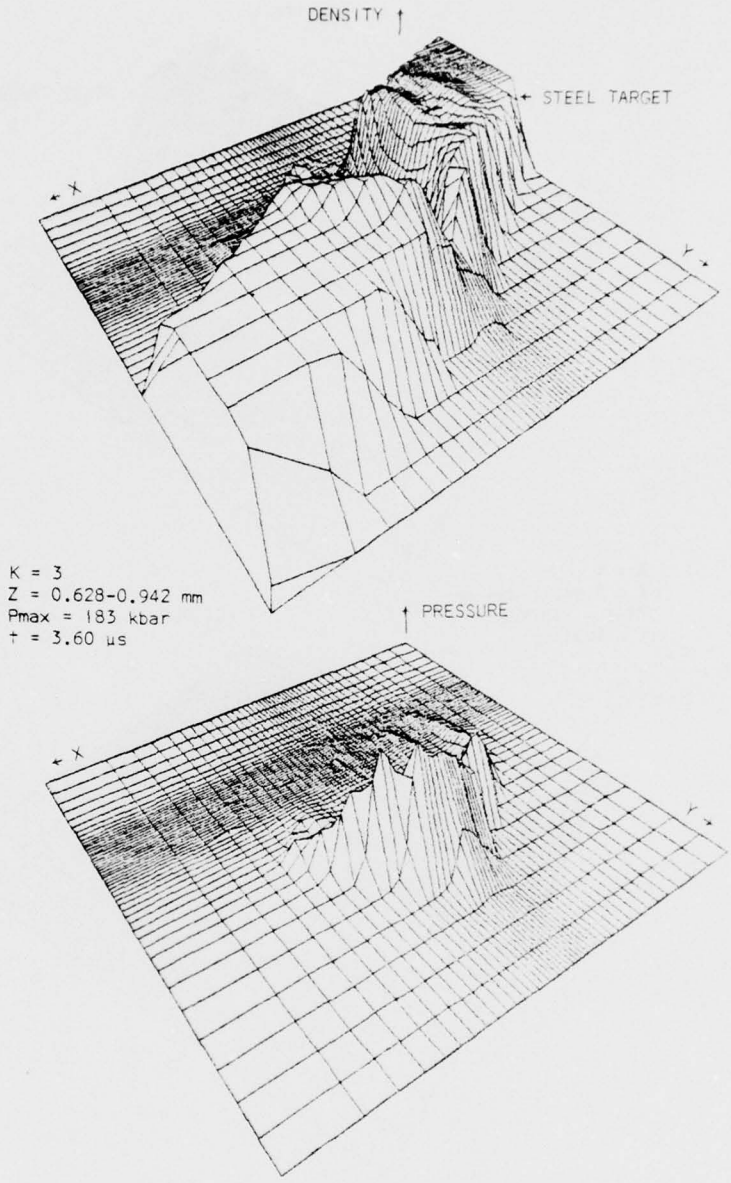

Figure 47. Density and Pressure Fields

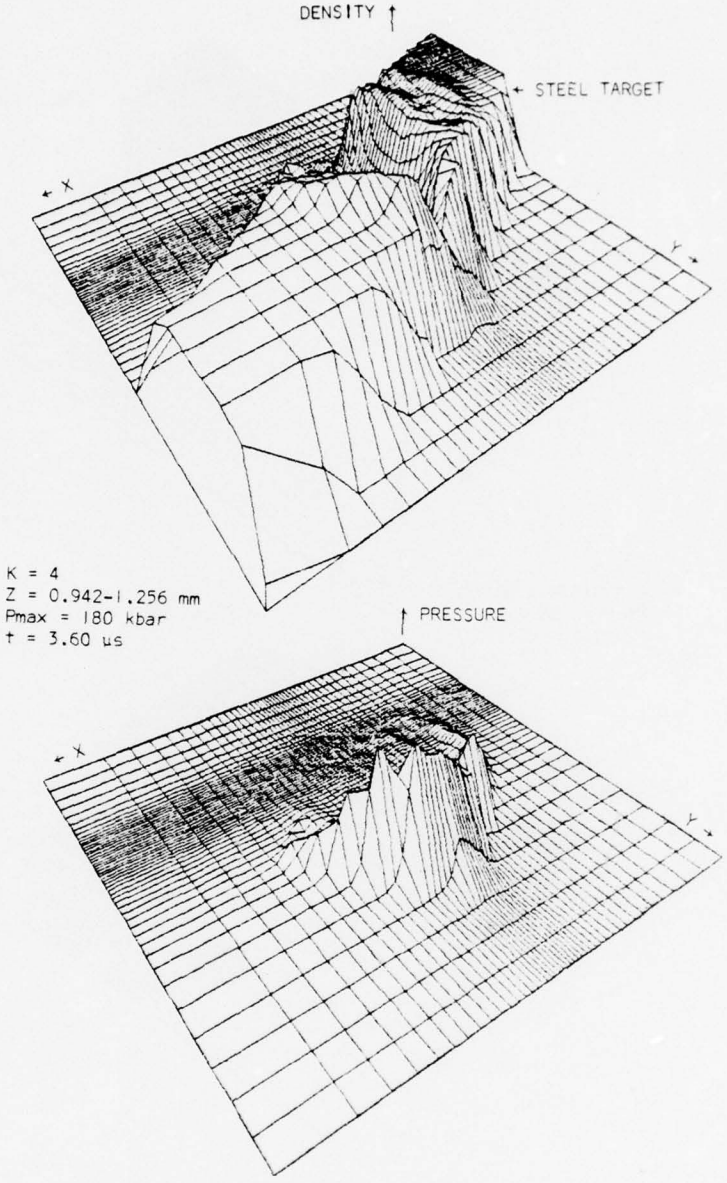

Figure 48. Density and Pressure Fields

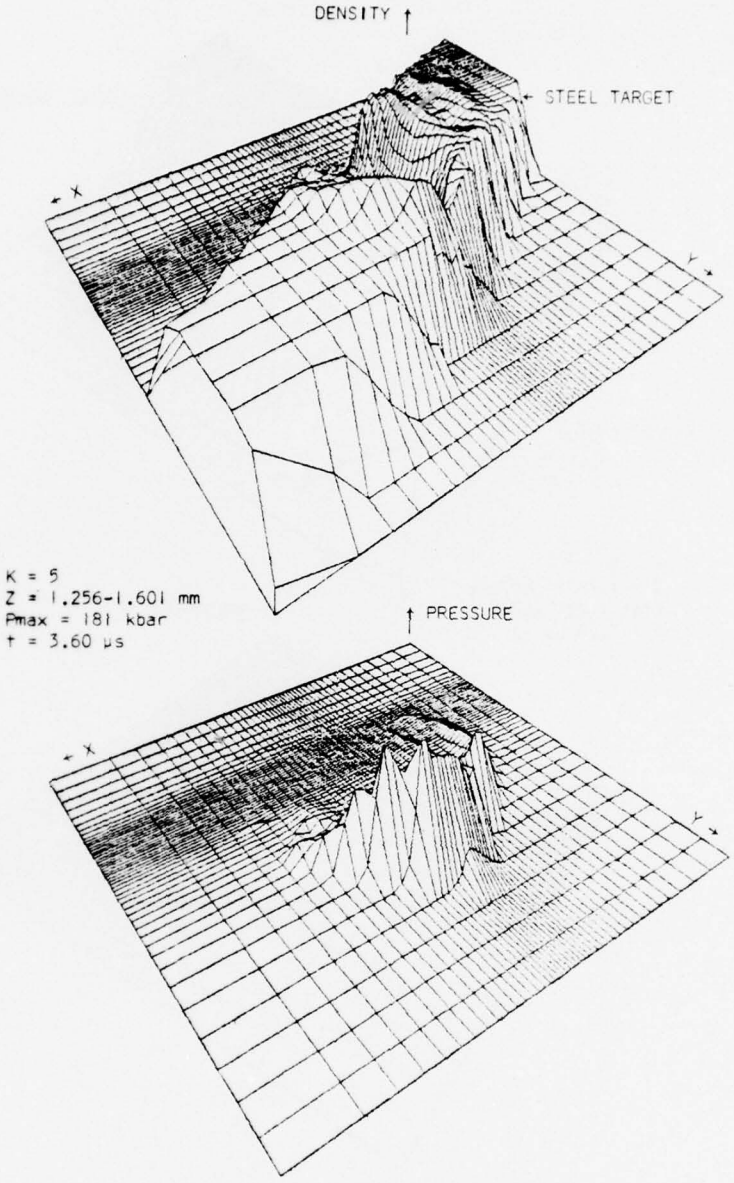

Figure 49. Density and Pressure Fields

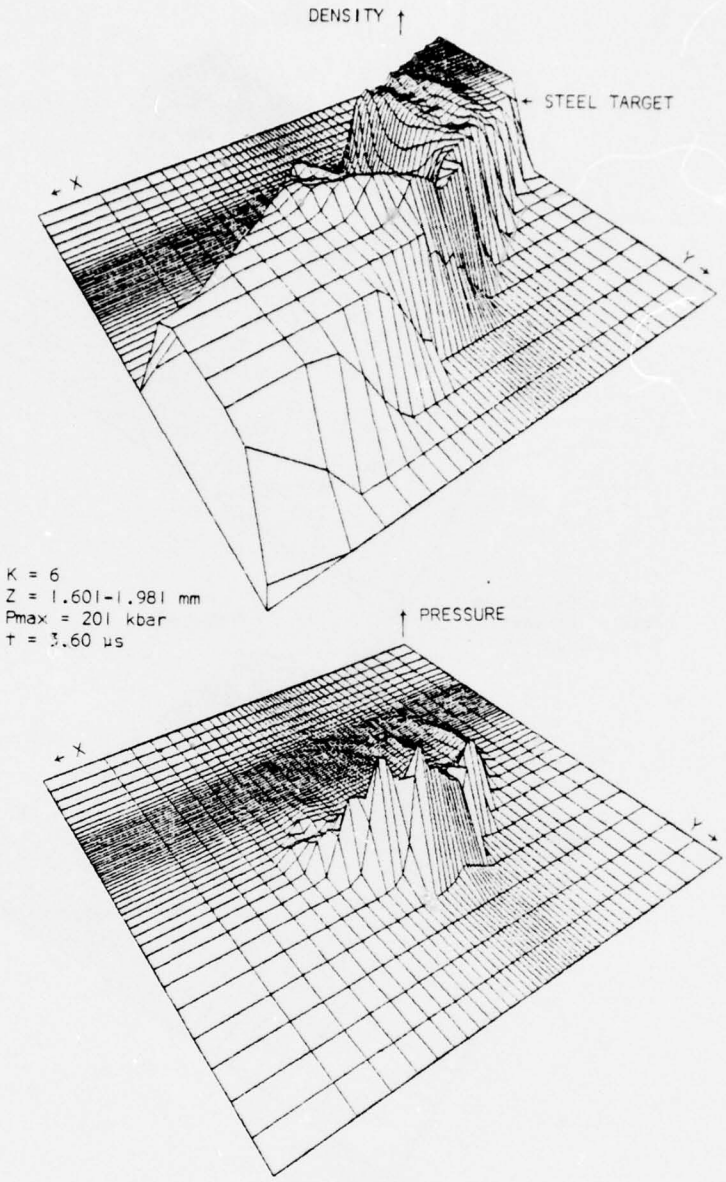

Figure 50. Density and Pressure Fields

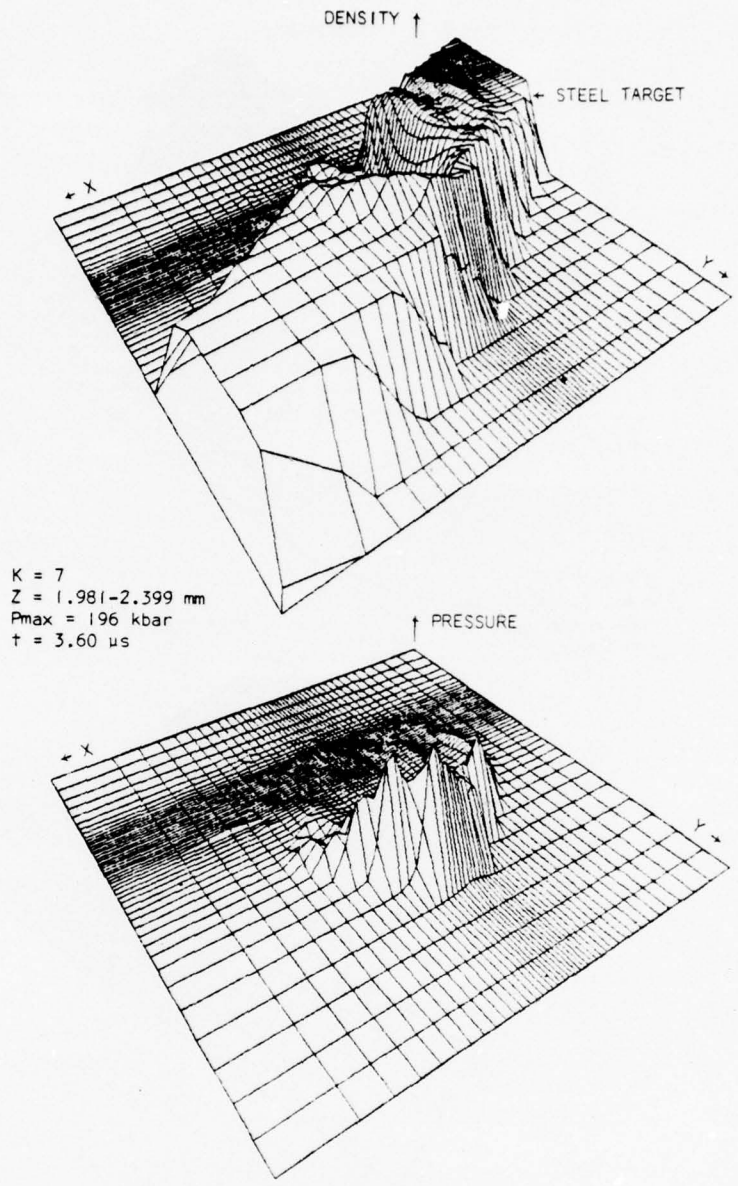

Figure 51. Density and Pressure Fields

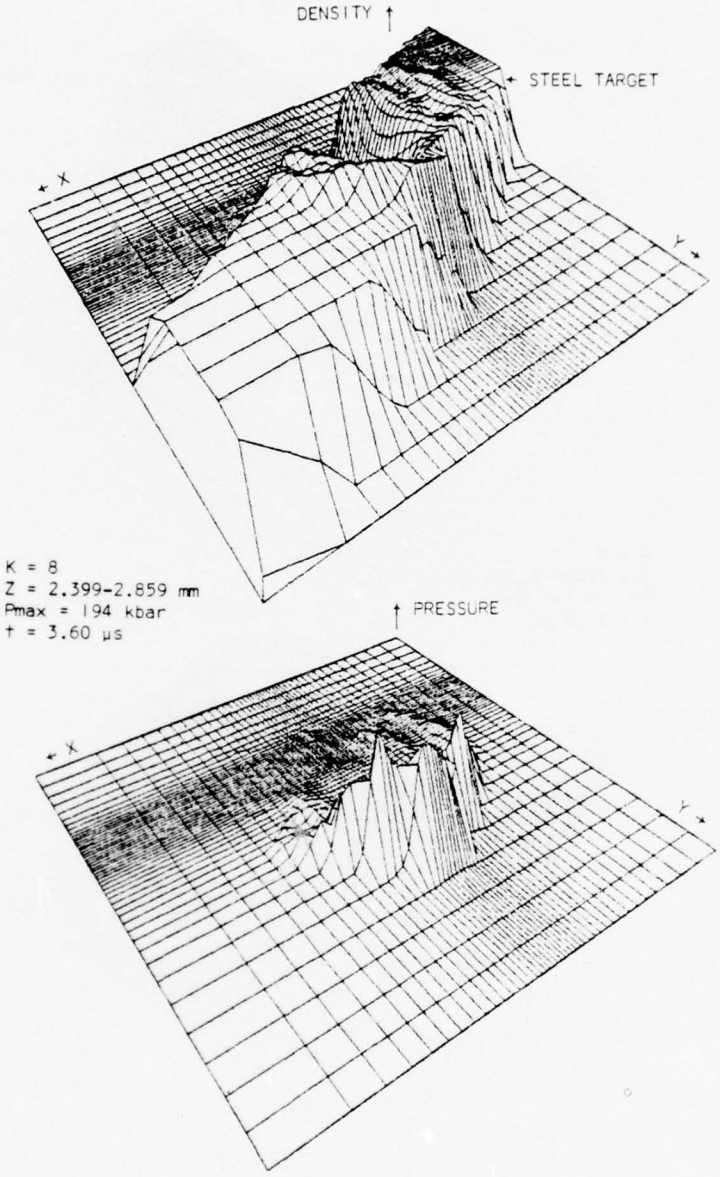

Figure 52. Density and Pressure Fields

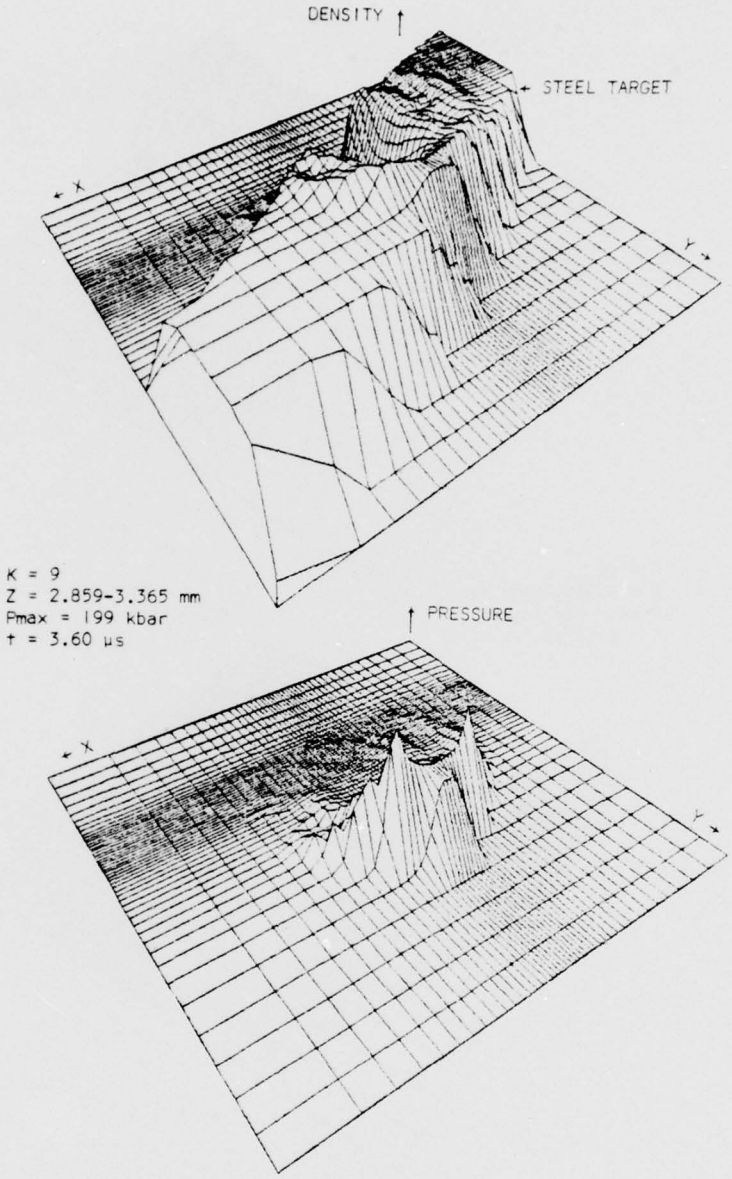

Figure 53. Density and Pressure Fields

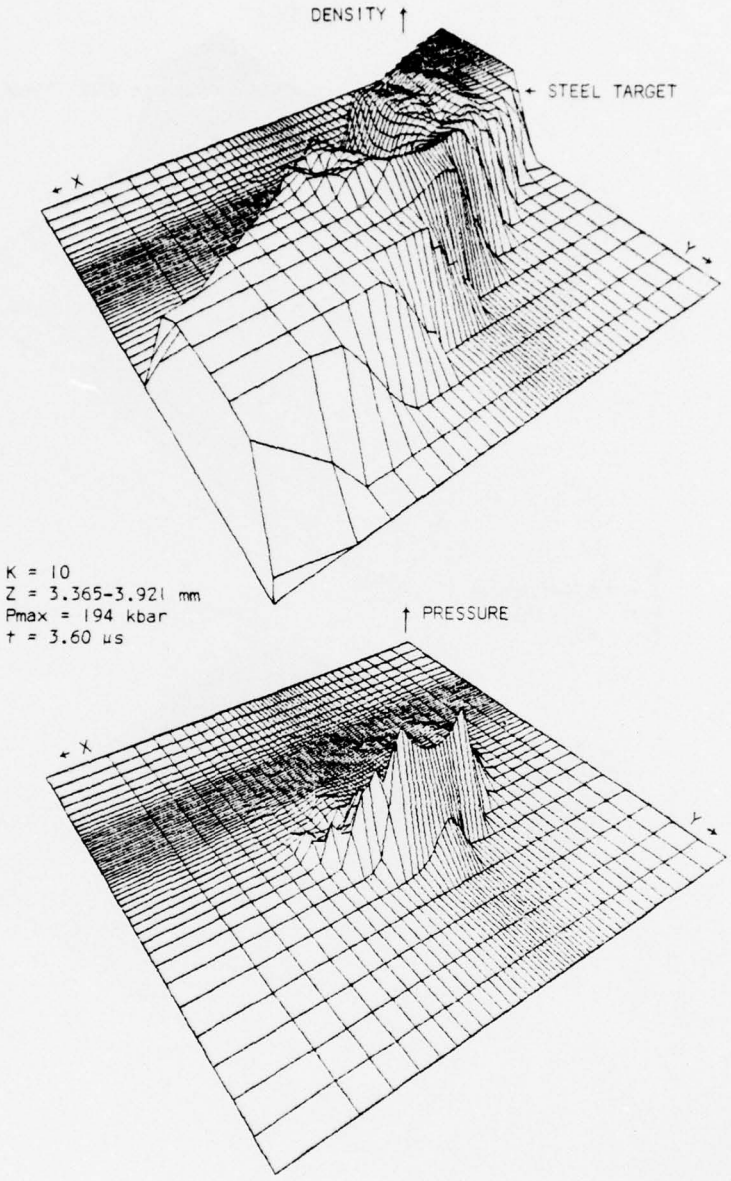

Figure 54. Density and Pressure Fields

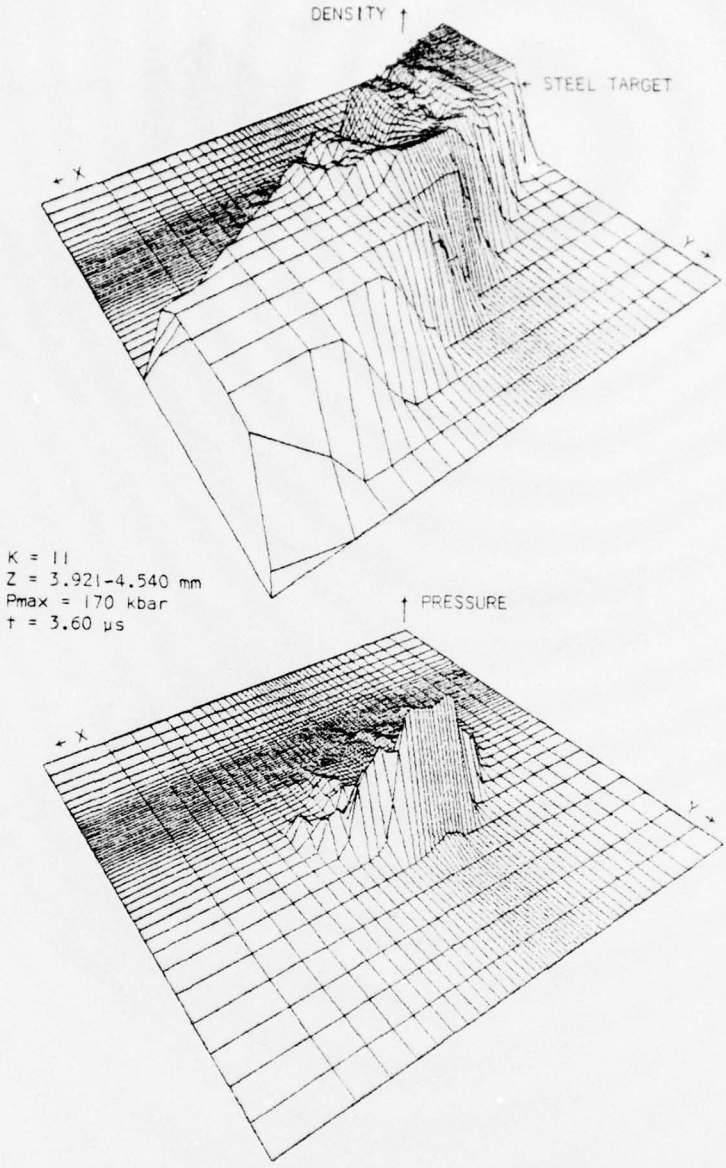

Figure 55. Density and Pressure Fields

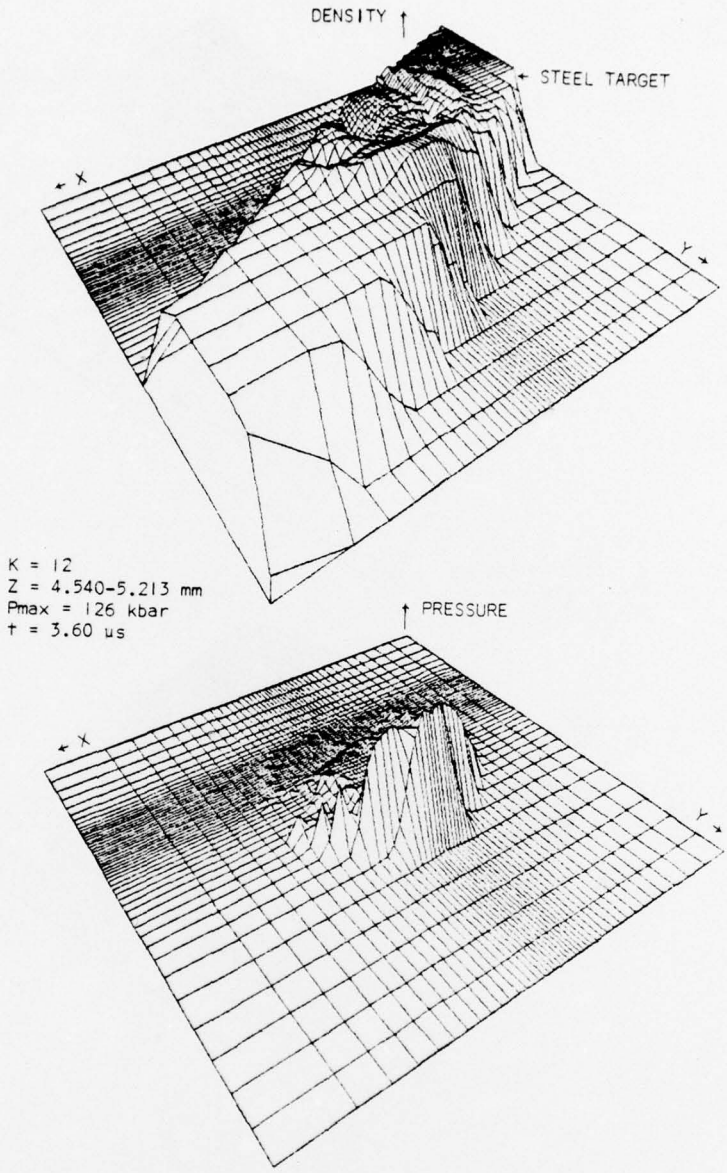

Figure 56. Density and Pressure Fields

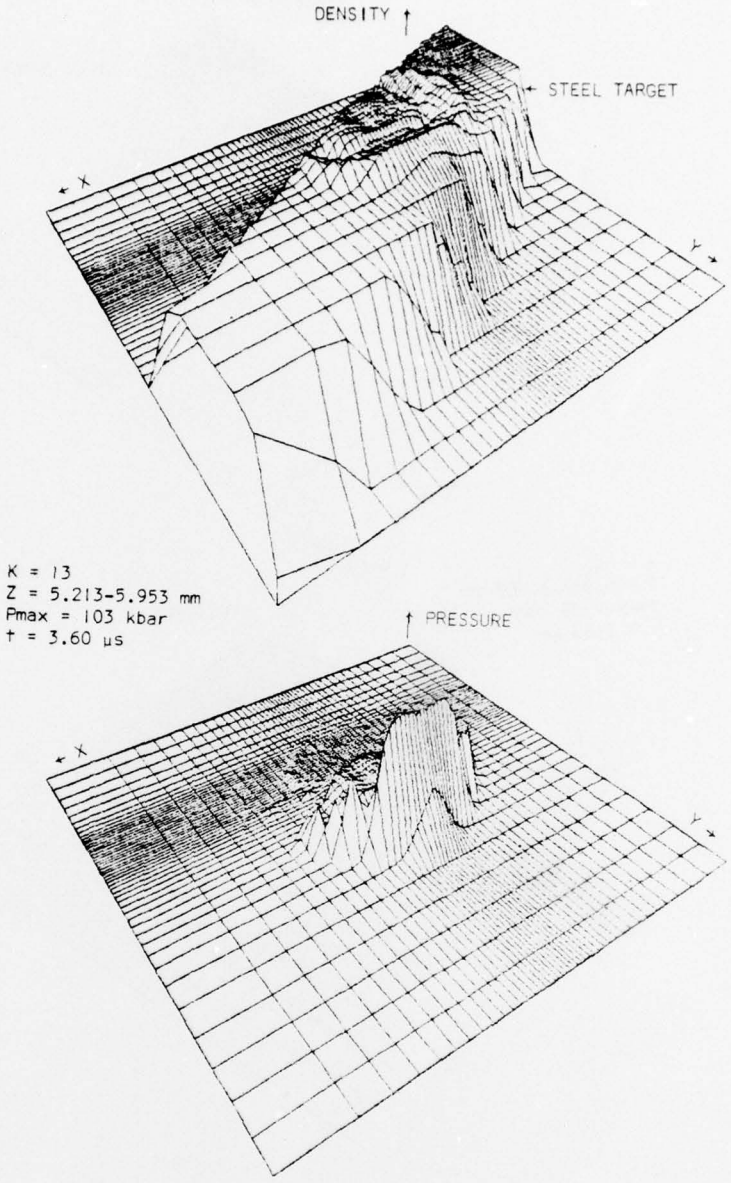

Figure 57. Density and Pressure Fields

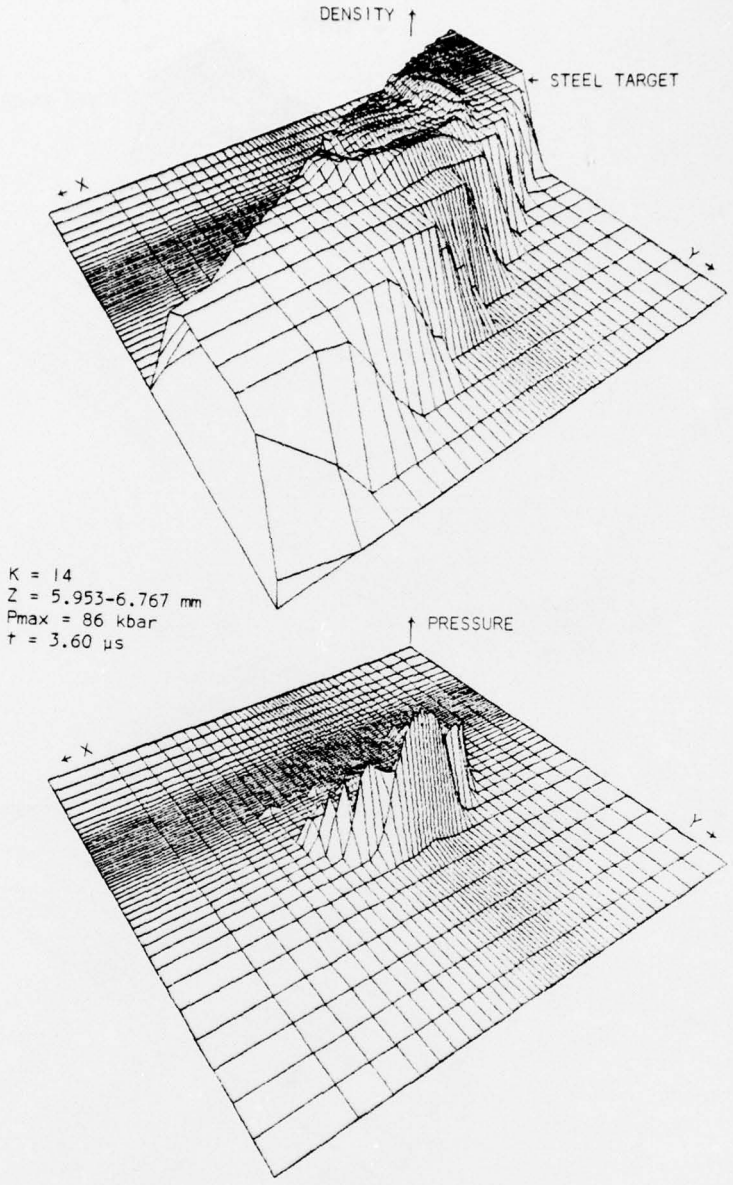

Figure 58. Density and Pressure Fields

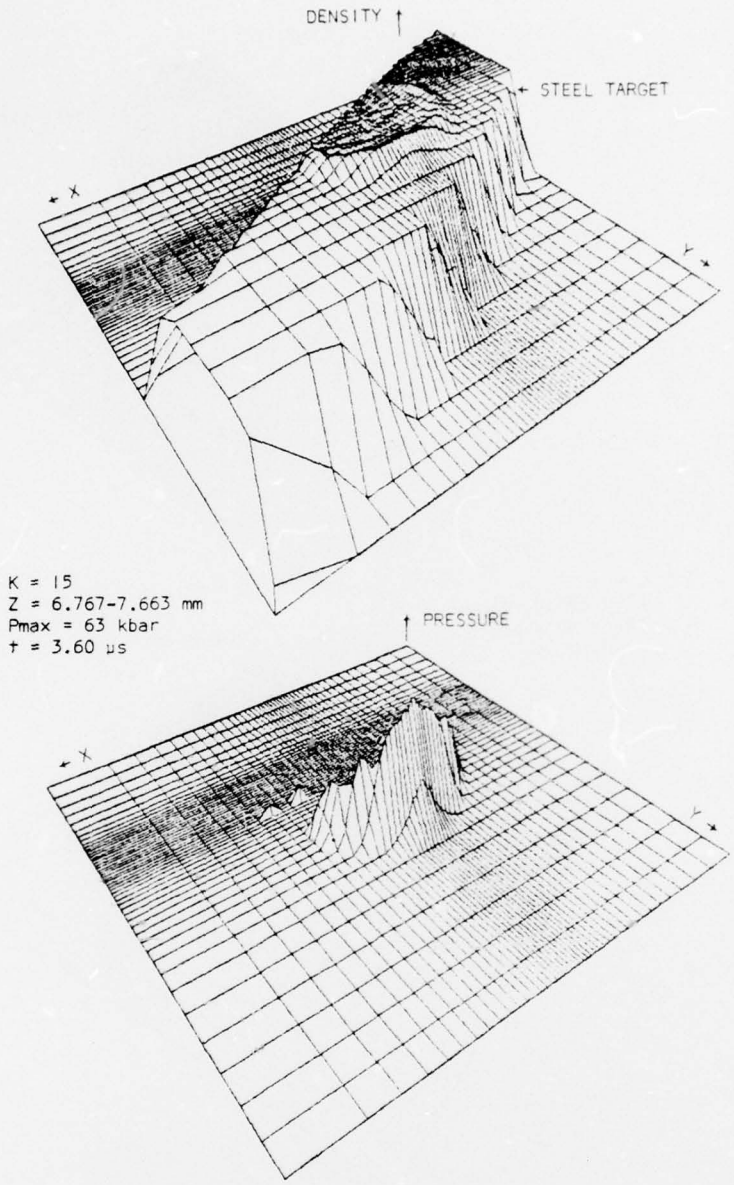

Figure 59. Density and Pressure Fields

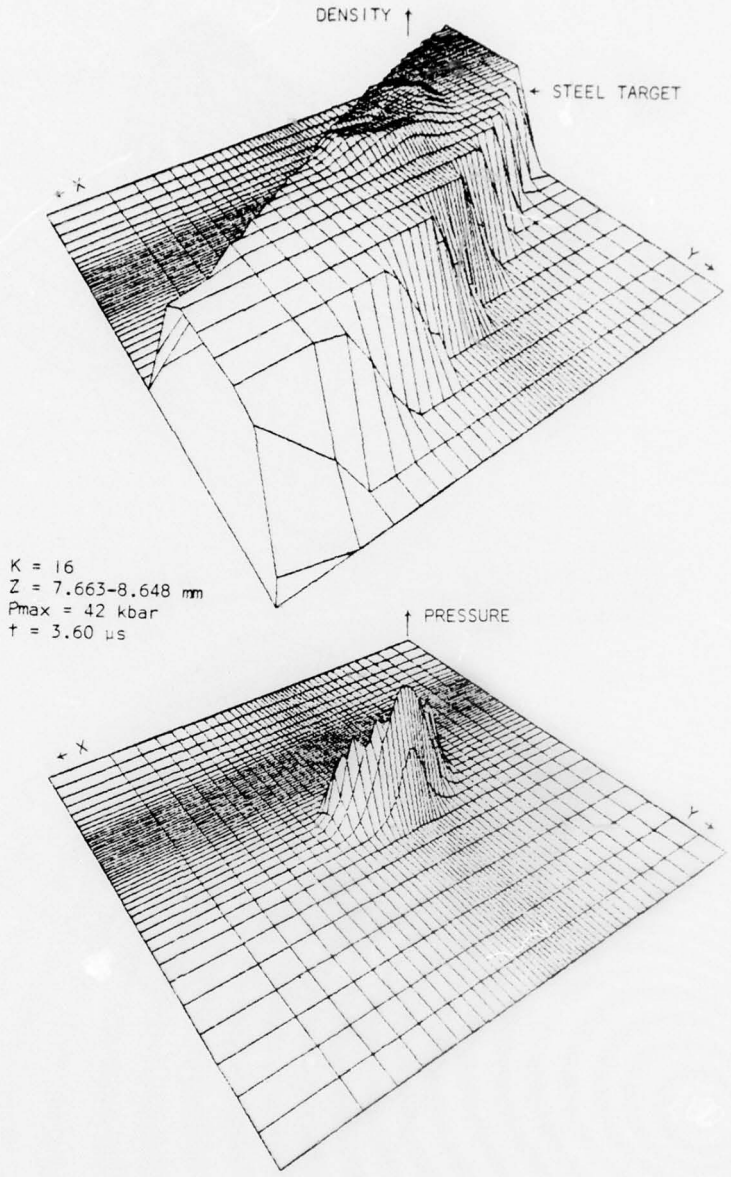

Figure 60. Density and Pressure Fields

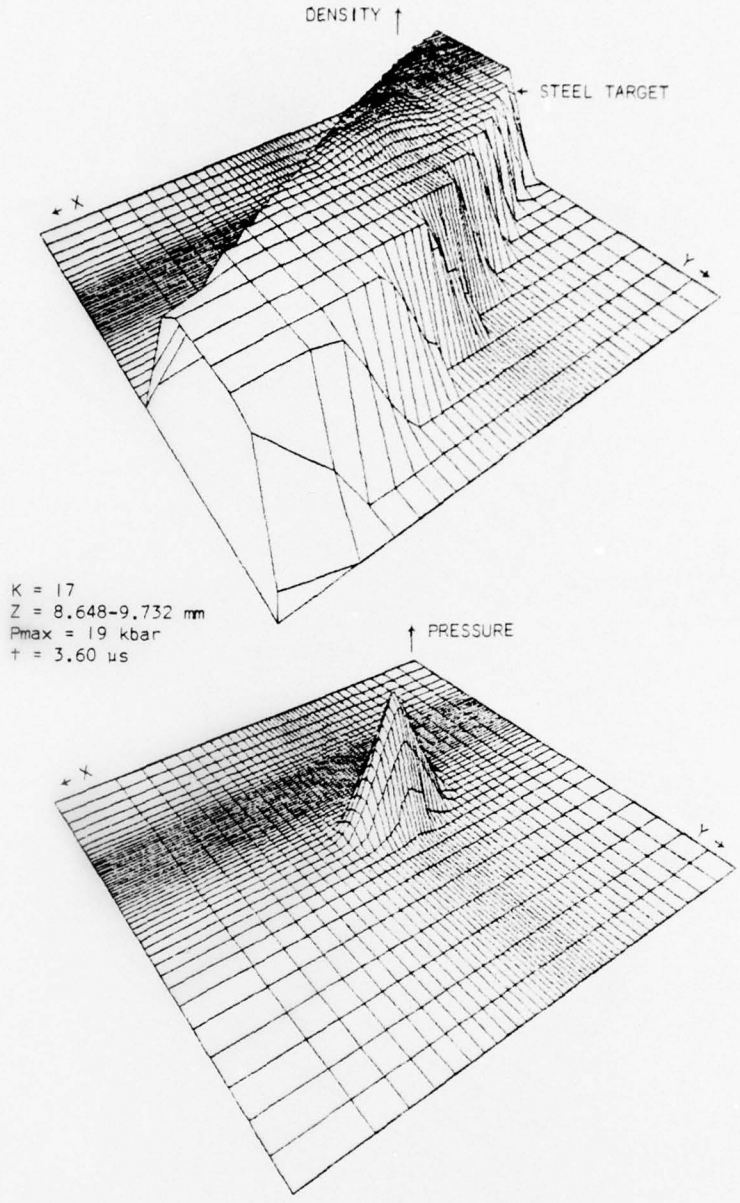

Figure 61. Density and Pressure Fields

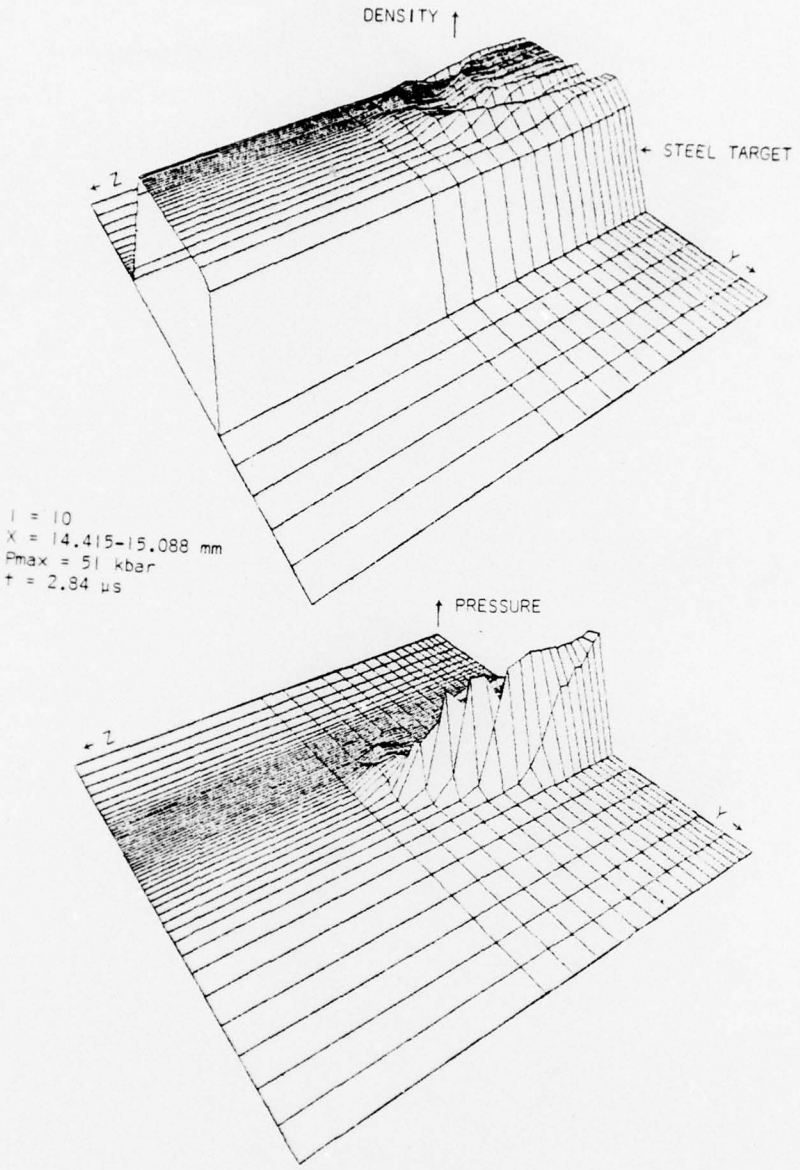

Figure 62. Density and Pressure Fields

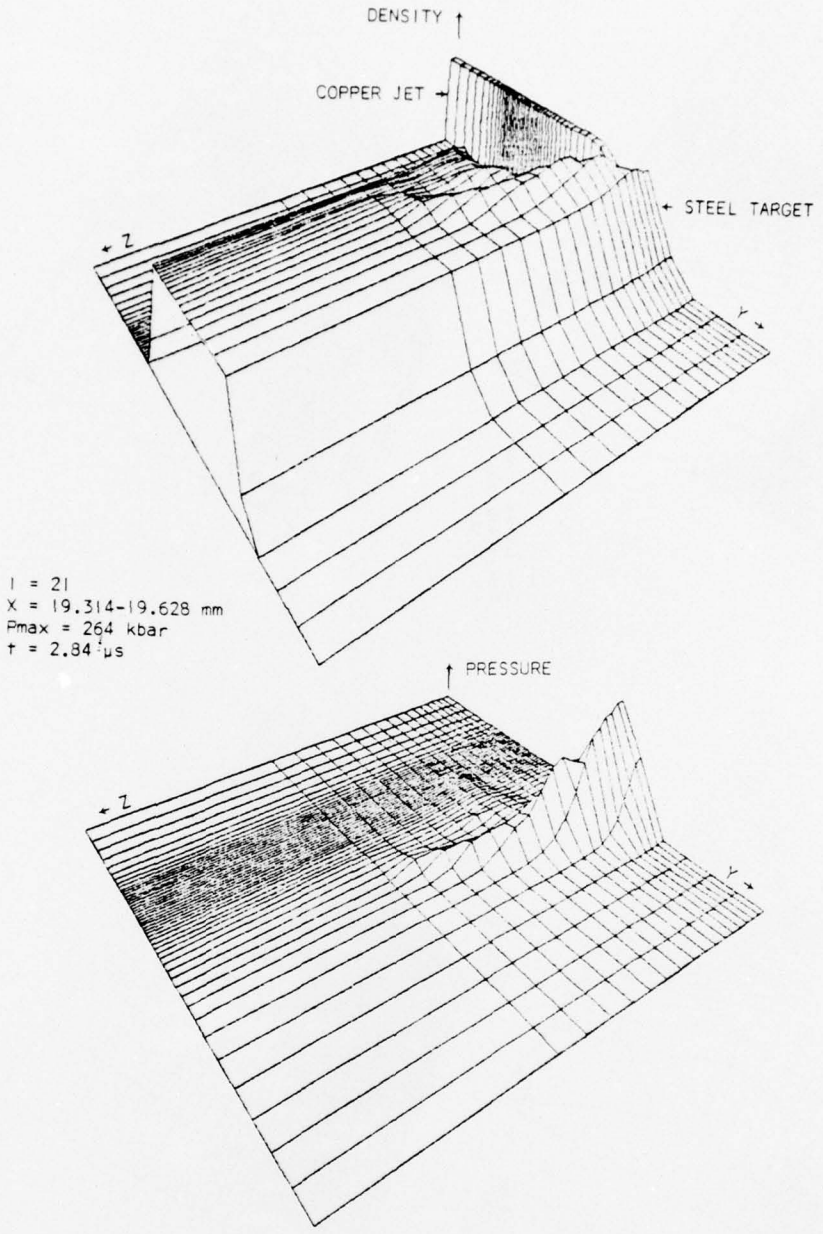

Figure 63. Density and Pressure Fields

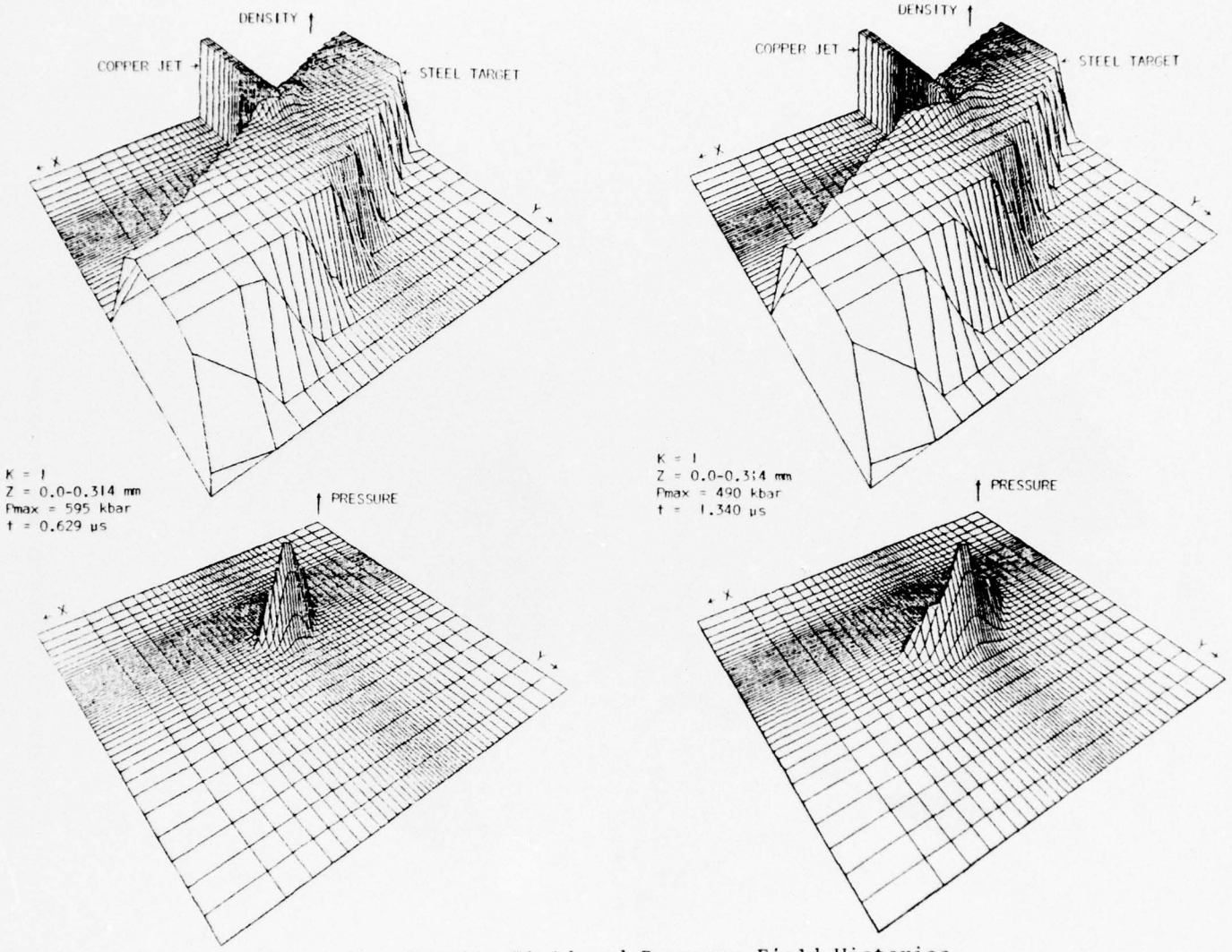

Figure 64. Density Field and Pressure Field Histories

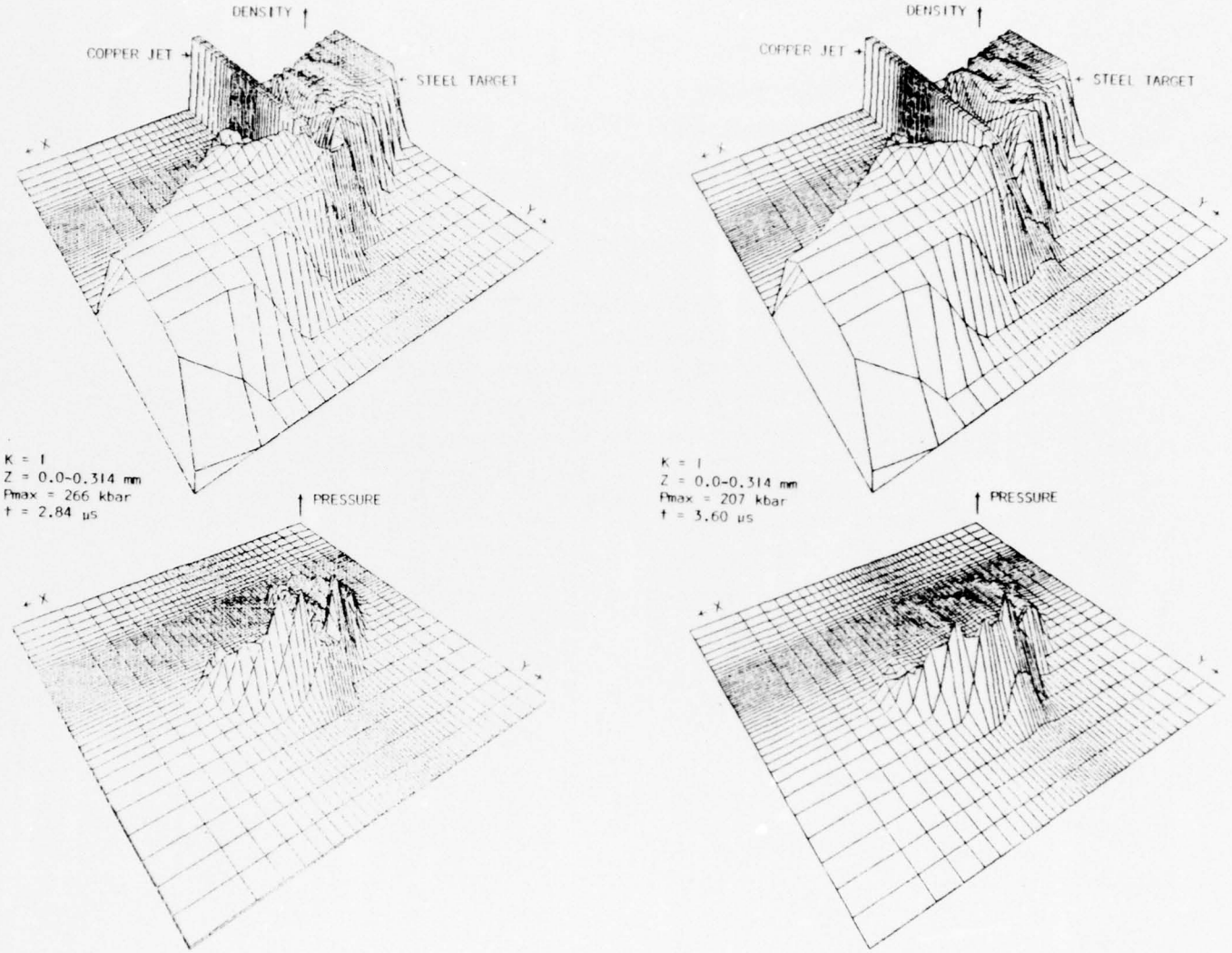

Figure 65. Density Field and Pressure Field Histories

DISTRIBUTION LIST

No. of Copies	Organization
12	Commander Defense Documentation Center ATTN: DDC-TCA Cameron Station Alexandria, VA 22314
1	Commander US Army Materiel Development and Readiness Command ATTN: DRCDMA-ST 5001 Eisenhower Avenue Alexandria, VA 22333
1	Commander US Army Aviation Systems Command ATTN: DRSAV-E 12th and Spruce Streets St. Louis, MO 63166
1	Director US Army Air Mobility Research and Development Laboratory Ames Research Center Moffett Field, CA 94035
1	Commander US Army Electronics Command ATTN: DRSEL-RD Fort Monmouth, NJ 07703
1	Commander US Army Missile Research and Development Command ATTN: DRDMI-R Redstone Arsenal, AL 35809
1	Commander US Army Armament Materiel Readiness Command Rock Island, IL 61202
2	Commander US Army Armament Research and Development Command ATTN: Mr. J. Pearson Tech Lib Dover, NJ 07801
1	Commander US Army Harry Diamond Labs ATTN: DRXDO-TI 2800 Powder Mill Road Adelphi, MD 20783
1	Commander US Army Materials and Mechanics Research Center ATTN: Tech Lib Watertown, MA 02172
1	Director US Army TRADOC Systems Analysis Activity ATTN: ATAA-SA White Sands Missile Range NM 88002
1	Assistant Secretary of the Army (R&D) ATTN: Asst for Research Washington, DC 20310
1	Director US Army BMD Advanced Technology Center ATTN: Mr. Price Boyd, BMDATC-M P. O. Box 1500 Huntsville, AL 35809
2	Chief of Naval Research ATTN: Code 427 Code 470 Department of the Navy Washington, DC 20325

DISTRIBUTION LIST

No. of Copies	Organization
2	Commander US Naval Air Systems Command ATTN: Code AIR-310 Code AIR-350 Washington, DC 20360
1	Commander US Naval Ordnance Systems Command ATTN: ORD-0332 Washington, DC 20360
1	Commander US Naval Surface Weapons Center ATTN: Tech Lib Dahlgren, VA 22448
1	Commander US Naval Surface Weapons Center ATTN: Code 730, Lib Silver Spring, MD 20910
1	Commander US Naval Weapons Center ATTN: Code 45, Tech Lib China Lake, CA 93555
1	Commander US Naval Research Laboratory ATTN: Code 7780, Walt Atkins 4555 Overlook Avenue Washington, DC 20375
1	USAF (AFRDDA) Washington, DC 20330
1	AFSC (SDW) Andrews AFB Washington, DC 20331
1	US Air Force Academy ATTN: Code FJS-RL (NC) Tech Lib Colorado Springs, CO 80940
1	Commander ATTN: Code OOAMA (MMECB) Hill AFB, UT 84401
1	AFWL (SUL) Kirtland AFB, NM 87116
1	AFLC (MMWMC) Wright-Patterson AFB, OH 45433
1	AFAL (AVW) Wright-Patterson AFB, OH 45433
1	Director National Aeronautics and Space Administration Langley Research Center Langley Station Hampton, VA 23365
1	Director Lawrence Radiation Laboratory ATTN: Mr. M. Wilkins P. O. Box 808 Livermore, CA 94550
2	Director Lawrence Livermore Laboratory K. Division ATTN: Dr. Mary Cunningham Mr. Jeff Thomsen P. O. Box 808 Livermore, CA 94550
1	Computer Code Consultants ATTN: Mr. M. Johnson 527 Glencrest Drive Solana Beach, CA 92075
1	Del Mar Technical Associates ATTN: Dr. Joel Sweet P. O. Box 1083 Del Mar, CA 92014

DISTRIBUTION LIST

No. of Copies	Organization
1	Physics International Corp ATTN: Mr. L. Berhman 2700 Merced Street San Leandro, CA 94577
1	Sandia Laboratories ATTN: Dr. L. Bertholf Albuquerque, NM 87115
1	Systems, Science and Software ATTN: Dr. R. Sedgwick P. O. Box 1620 La Jolla, CA 92037
1	Drexel Institute of Technology Wave Propagation Research Ctr ATTN: Prof. P. Chou 32nd & Chestnut Streets Philadelphia, PA 19104
2	University of California Los Alamos Scientific Lab ATTN: Dr. J. M. Walsh Tech Lib P. O. Box 1663 Los Alamos, NM 87545
	Aberdeen Proving Ground
	Marine Corps Ln Ofc Dir, USAMSAA